Report number 5637

# Experimental Slip-based Road Condition Estimation

Niklas Petersson and Martin Santesson

February 11, 2000

Advisor at Lund Institute of Technology:
Professor Anders Rantzer

Advisor at University of California, Berkeley:
Professor J. Karl Hedrick

Department of Automatic Control
Lund Institute of Technology

Department of Mechanical Engineering
University of California at Berkeley

## Abstract

Heavy traffic loads on the California highways have given birth to the development of automated highways. With vehicles traveling without human interaction, tighter spacing between cars can be achieved without jeopardizing safety, leading to improved highway throughput. Since no human driver is present to make judgements about velocity and spacing, knowing the road condition is important in order to maintain safety.

This project aims to, based on experimental measurements, give information about the road condition, and in this thesis a slip-based method is used. Slip is defined as the relative difference in velocity between the wheels and the vehicle.

The data acquired from a Lincoln Towncar introduced difficulties due to very noisy measurements. A number of different approaches of extracting road surface information from the noisy slip data was examined and an observer was developed that significantly reduced unwanted effects caused by tire elasticity.

The resulting road classifier could distinguish between dry and wet asphalt roads with 16% error probability. The classifier did only work for newly wet roads, most likely since roads are known to be the most slippery right after it has started to rain.

## Preface

We worked on our Master's thesis project in the Department of Mechanical Engineering at the University of California, Berkeley during the fall semester 1999.

Thanks to Michael Uchanski for his guidance and enthusiasm throughout the project, and to Rick Hill for helping us out with the experimental work. We would also like to thank our advisors, professor Anders Rantzer for initiating the contact with UC Berkeley, and professor J. Karl Hedrick for giving us the opportunity to work on our project in his lab.

Thanks to Stiftelsen AF, Ernhold Lundströms Stiftelse and Hakon Hanssons Stiftelse for financial aid.

# Contents


**1 Introduction** **7**
- 1.1 Background . . . 7
- 1.2 Project formulation . . . 7
  - 1.2.1 The big picture . . . 9
- 1.3 Outline of the report . . . 9

**2 Slip and Car Dynamics** **11**
- 2.1 Slip . . . 11
  - 2.1.1 Definition of slip . . . 12
  - 2.1.2 Slip curve characteristics . . . 12
  - 2.1.3 Magic formula . . . 13
  - 2.1.4 Slip offset . . . 13
- 2.2 Car dynamics . . . 14

**3 Measuring Road Conditions** **17**
- 3.1 Visual methods . . . 17
- 3.2 In Tire sensors . . . 17
- 3.3 Slip approach . . . 17
  - 3.3.1 Acceleration . . . 18
  - 3.3.2 Deceleration . . . 18

**4 Experimental Setup** **19**
- 4.1 The car . . . 19
  - 4.1.1 Brake system . . . 19
  - 4.1.2 Sensors . . . 19
  - 4.1.3 Data acquisition . . . 21
- 4.2 Test track . . . 22

**5 Chosen Approach** **23**
- 5.1 Choice of slip-based method . . . 23
- 5.2 Choice between acceleration and deceleration . . . 23

**6 Experimental Considerations** **25**
6.1 Need of reference speed . . . . . 25
6.2 Choice of wheels used for braking . . . . . 26
6.3 Road surfaces . . . . . 27
6.4 Test profiles . . . . . 27
6.4.1 The need of road force excitation . . . . . 27
6.4.2 Automatic driving . . . . . 27
6.4.3 Manual driving . . . . . 28

**7 Slip Estimation** **31**
7.1 Choice between speed measurements . . . . . 31
7.1.1 Wheel speed signals . . . . . 31
7.1.2 The *high* and *divide* signals . . . . . 32
7.1.3 Improving the *divide* signal . . . . . 32
7.1.4 Comparing the accuracy of different measurements . . 33
7.1.5 Choice of which measurements to use . . . . . 34
7.2 Noise characteristics . . . . . 34

**8 Road Force Estimation** **37**
8.1 Using acceleration . . . . . 37
8.2 Using brake pressure . . . . . 37

**9 Classification Part I** **39**
9.1 Initial tests . . . . . 39
9.2 Linear curve fitting . . . . . 40
9.2.1 Least squares fitting of a line . . . . . 40
9.2.2 Averaging over the slip axis . . . . . 41
9.2.3 Calculating the offset before the slope . . . . . 42
9.3 Curve fitting to functions capturing the slip curve essentials . 42
9.3.1 Using the Pacejka–Bakker tire model . . . . . 43
9.3.2 Using a polynomial . . . . . 43

**10 Simulation Model** **45**
10.1 Top level model . . . . . 46
10.2 Wheel modeling . . . . . 46
10.3 Suspension modeling . . . . . 47
10.4 Decelerating forces . . . . . 48
10.4.1 Rolling resistance . . . . . 48
10.4.2 Drag force . . . . . 48
10.4.3 Implementing a simulation model . . . . . 48
10.5 Running the simulations . . . . . 48
10.5.1 Braking input . . . . . 49
10.5.2 Simulation of different surfaces . . . . . 49

**11 Recursive Slip Slope Estimation** **51**
11.1 Model . . . . . 51
11.2 The Kalman filter . . . . . 52
11.2.1 The general case . . . . . 52
11.2.2 The recursive slip slope estimator . . . . . 53
11.3 Decision variable . . . . . 54
11.4 Differences to previous work . . . . . 54

**12 Elastic Wheel Observer** **55**
12.1 Modeling the behavior . . . . . 56
12.1.1 Function of the vehicle speed . . . . . 56
12.1.2 Change in tire radius . . . . . 56
12.1.3 Elasticity of the wheel . . . . . 56
12.2 Simulation of the model . . . . . 58
12.3 Observer . . . . . 58
12.3.1 Observability and convergence . . . . . 59
12.3.2 Modification of the observer . . . . . 60
12.3.3 Discretizing the model . . . . . 61
12.3.4 Kalman gain for the observer . . . . . 61
12.3.5 Verifying the observer . . . . . 61

**13 Classification Part II** **63**
13.1 Putting it together . . . . . 63
13.2 Results . . . . . 64
13.2.1 Check maximum friction . . . . . 65
13.3 Classification . . . . . 67
13.3.1 Selecting a threshold between the surfaces . . . . . 67
13.3.2 Error probabilities . . . . . 68

**14 Conclusions** **69**
14.1 Results . . . . . 69
14.2 Problems — What could have been done different? . . . . . 70
14.3 Future work . . . . . 70

**Bibliography** **73**

# Chapter 1

# Introduction

## 1.1 Background

Due to heavy congestion problems on the California highways, there is an ongoing development of Automated Highway Systems, AHS. The goal is to automatically operate standard automobiles at highway speeds at close spacings. With precise automatic control there can be much tighter spacing between the vehicles than possible during manual driving. The tighter spacing enables the highway throughput to be at least twice what it is today [PAT]. Other benefits with vehicle platooning are that the aerodynamic drag forces are significantly reduced, resulting in less fuel consumption and reduced exhaust emissions. In a demonstration in 1997, eight Buick LeSabres drove on a section of a highway in San Diego without any driver interaction. The AHS project is conducted by California PATH, Partners for Advanced Transit and Highways, in which the University of California plays a large role. It is essential to have information about the road condition with such close spacings that the AHS require. If the road is slippery, wider spacing is necessary to maintain safety, on the other hand, too wide spacing will lead to lower capacity on the highways. Therefore it is important to have exact information about what maximum friction force the tire–road interface can supply.

The importance of knowing the state of the road is not just useful for the automated case. This kind of information would also assist a human driver making judgments about maintaining safe speed and sufficient distance to other cars during driving.

## 1.2 Project formulation

The goal is to classify different road surfaces, dry and wet, using available standard sensors on an automobile to the fullest possible extent. The purpose is to get information about how slippery the road is.

Figure 1.1: Demonstration of vehicle platooning.

A Lincoln Towncar was available for testing, equipped with sensors for measuring wheel speed, brake pressure and acceleration just to mention some.

The chosen approach is to use the friction dependency of the slip, to be able to distinguish between different road conditions. The slip, $\lambda$, is defined as the relative difference between the speed of the wheel and the car velocity. The formula looks like

$$\lambda = \frac{v - \omega r_w}{\max(\omega r_w, v)}, \tag{1.1}$$

where $\omega$ is the angular velocity of the wheel and $r_w$ is the radius. When plotting the slip versus the normalized friction force, $\mu$, the initial slip slope is different for different road surfaces. The slope of the slip can be used for categorizing different road conditions. The normalized friction force, or normalized road force, is equal to the road force acting on the tires divided by the normal force.

We decided to try to estimate the slip slope based on deceleration only. In order to obtain the slip, the velocity of the car has to be known, which causes a problem when all wheels are braking. To solve this, the front wheels were used for braking, while the rear wheels served to give reference speed for the car, assuming no slip on the rear wheels. Naturally, this approach is not feasible for practical use, when all four wheels are needed for braking. The assumption is made that in the future a velocity observer for the car will be developed that will enable the use of all four wheels for braking.

### 1.2.1 The big picture

Communication between cars in the automated highways is already existing. In a future perspective, communication between cars could mean that road condition information about a patch of road would not just benefit the car that happened to gather the information, but also all other cars soon passing over that very stretch of road. Every time a car does a braking maneuver it would send road condition information to a road-side computer which then would distribute this information to cars passing over that patch of road. With thousands of vehicles per hour traveling on the same road, an extensive map of the road conditions would be created. This would also mean that it would not be necessary for a car to process the collected raw data in real-time, since the information could benefit other vehicles, soon passing by. Naturally this kind of mapping of road conditions would be combined with weather reports to improve the reliability of the information.

## 1.3 Outline of the report

The basic theory of slip and car dynamics is described in chapter 2. Chapter 3 goes through a couple of different methods of measuring road conditions. Chapters 4 – 6 discuss the experimental setup we had, what the chosen approach was and the experimental considerations that had to be taken in order to get good results. The seventh and eighth chapter describe how the two slip curve axes, i.e. the slip and normalized road force, were obtained. Different ways of extracting the slip slope from the slip curves, in spite of noisy measurements, are discussed in chapter 9. The tenth chapter goes through the simulation model. Chapters 11 – 12 describe a more sophisticated way of extracting the slip slope, as well as a method of eliminating the effects of elasticity of the tire in the slip measurements. Chapter 13 combines the previously mentioned methods into a road surface classifier. Finally, the fourteenth chapter discusses the results obtained, things that could have been done differently and makes suggestions for future work.

# Chapter 2

# Slip and Car Dynamics

## 2.1 Slip

In the contact surface between the tire and the road, a friction force is acting. This force will build up a slip, which is the relative difference between the speed of the wheel and the speed of the vehicle.

During acceleration, the driving wheels will rotate slightly faster than the driven wheels, which rotate in the same speed as the car. During braking, the situation is the same, except for that the wheels now rotates slower than the car moves. One way to explain that the wheel can have a different angular velocity than the car is looking at the compression of the tire in the tire–road contact region. During acceleration, the compression is as shown in figure 2.1. Before entering the contact region, the tire tread is compressed.

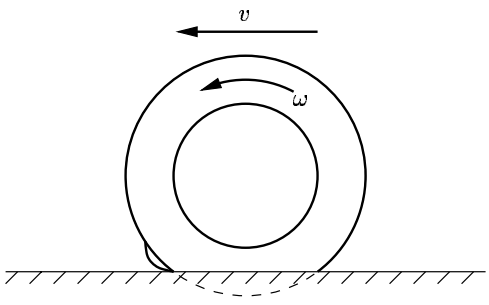


Figure 2.1: Compression of the tire, generating slip.

The distance the tire rolls will become smaller than if free rolling was the case.

### 2.1.1 Definition of slip

As mentioned, the slip, $\lambda$, is defined as the relative difference in speed between the wheel and the car velocity. In this report, positive slip occurs during braking and negative during acceleration.

$$\lambda = \frac{v - \omega r_w}{\max(\omega r_w, v)} \tag{2.1}$$

In one of the extreme cases, when the wheel has locked up and $\omega = 0$, the slip will be $\lambda = +1$. When the wheel is spinning without the car moving, the slip will become $\lambda = -1$.

### 2.1.2 Slip curve characteristics

The friction force from the road is what accelerates or decelerates the car, if drag force is neglected. The normalized friction force is defined as

$$\mu = \frac{F_{road}}{N}, \tag{2.2}$$

where $F_{road}$ is the road friction force and $N$ is the normal force of one wheel.

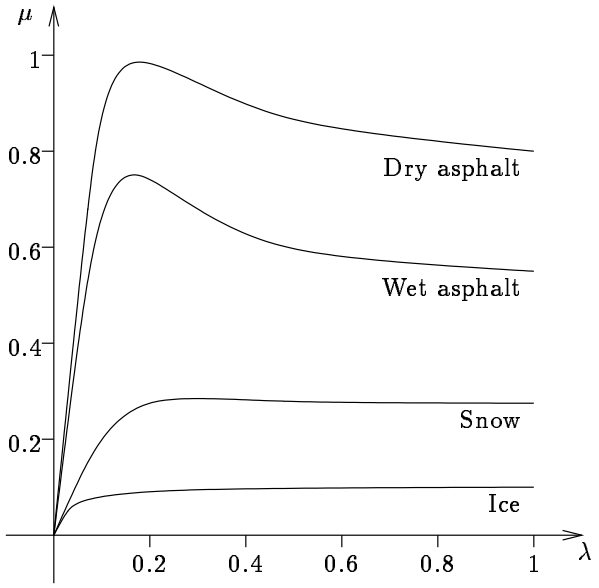


Figure 2.2: Schematic plot of slip curves for different surfaces. However not shown here, the slip curves are mirrored into the third quadrant for negative slip.

The slip and friction coefficient can be plotted together as a slip curve. These curves are different for different surfaces as can be seen in figure 2.2.

The slip curve typically reaches its maximum value below 20% slip. If this slip value is exceeded, the force decreases. As it decreases, the slip increases even more. This causes an instable situation, and the slip increases until it reaches its maximum value, $\lambda = \pm 1$, which corresponds to spinning or skidding.

Looking at the different curves, one can see that they have different peak values of friction force. This means that they can support different levels of braking or acceleration.

The final value of the force, which occurred with maximum slip, is somewhat smaller than the peak value. This can be compared to static and dynamic friction when pushing an object over a surface. The static friction can reach a higher value before the object starts moving than the dynamic friction can when the object is sliding, and that is the same phenomena as here.

As seen in figure 2.2, different surfaces have both different peak values and different slopes of the curve in the beginning.

If the maneuvers are not purely in the longitudinal direction, as acceleration or deceleration, there will also be lateral forces affecting the tires. This will cause a side slip similar to the longitudinal slip. When the lateral forces increase, the maximum longitudinal force decreases, and the slip curves in figure 2.2 will have lower $\mu$ values.

### 2.1.3 Magic formula

It is not easy to assign a function to a slip curve, but there exist empirical approximations of the curves. One is the Pacejka-Bakker Magic Formula [YJ98],

$$F(\lambda) = D \sin\left(C \arctan\left(B\lambda - E\left(B\lambda - \arctan(B\lambda)\right)\right)\right). \tag{2.3}$$

With the right parameters this equation is a good approximation of the real look of the slip curve.

### 2.1.4 Slip offset

When looking at real data from measurements, it can be seen that the slip curves do not start in the origin. There seems to be an offset generating slip even if there are no road forces.

One reason of this is the way measurements are carried out in the vehicle. Due to the rolling resistance and drag force, there are external forces that can be hard to get a measurement of.

Another reason is that the different wheels can have different radii. If you have one wheel giving the reference speed of the vehicle and that wheel is bigger than the wheel for which you want to calculate the slip, you will get a slip that is similar to what you would get during a braking maneuver.

## 2.2 Car dynamics

The movements of the car in the three dimensions are shown in figure 2.3. Yaw, pitch and roll are angles corresponding to rotations around each of the axes.

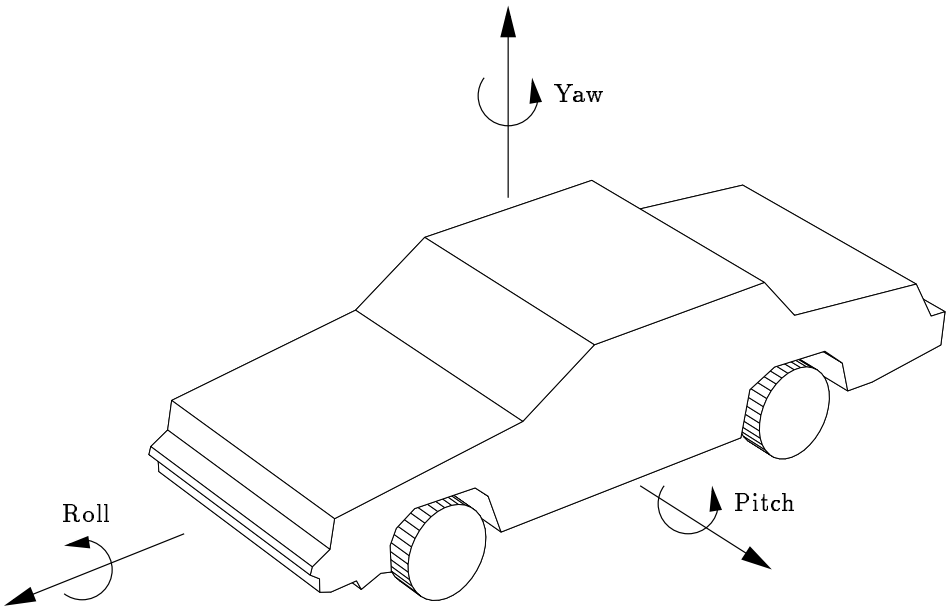


Figure 2.3: Definition of yaw, pitch and roll.

The dynamics of the wheel are shown in figure 2.4. The angular velocity of the wheel, $\omega$, is given by

$$J\dot{\omega} = \tau - F_{road}r, \tag{2.4}$$

where $J$ is the moment of inertia of the wheel and $\tau$ is the sum of the brake torque and for the driving wheels also the drive line torque.

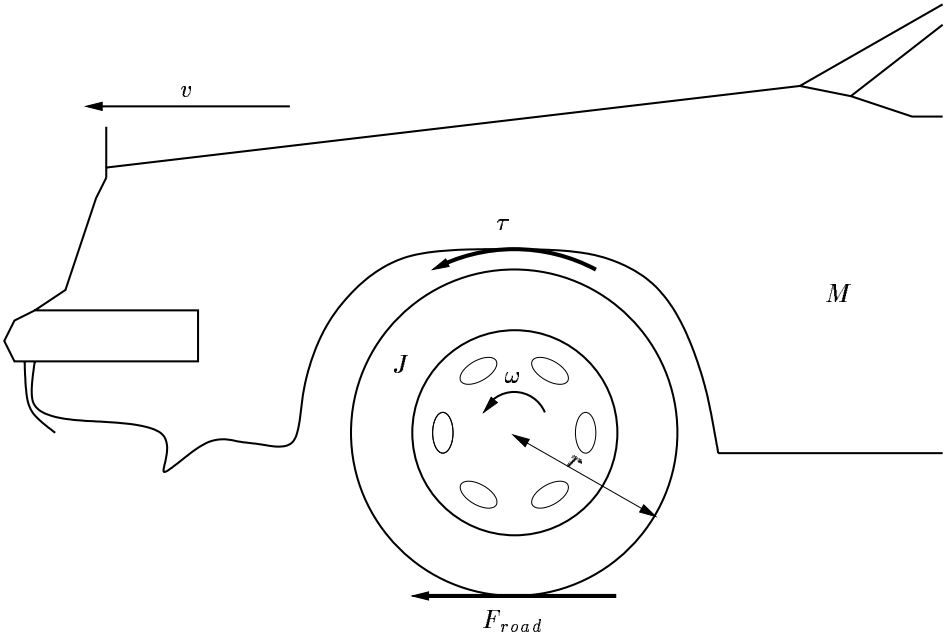


Figure 2.4: Dynamics of the wheel.

# Chapter 3

# Measuring Road Conditions

This chapter will describe some of the different methods used to categorize different road surfaces.

## 3.1 Visual methods

The concept of the visual methods is to expose the road surface to a light and measure the spectrum of the reflected light, as well as the intensity. By using this information it is possible to draw conclusions about the coarseness and reflectivity of the road, which then can be used for distinguishing between different road surfaces [USY94]. One nice feature with this method is that a slippery road patch can be detected before actually driving on it, if the light source is mounted in the front of the vehicle. Drawbacks of this method are the requirement of additional sensors as well as problems with keeping the lens clean.

## 3.2 In Tire sensors

It is possible to vulcanize sensors in the tread elements of the tire for measuring stress and strain. This is done in [BER92] using a magnetic sensor. The method is technically very complicated and expensive.

## 3.3 Slip approach

The friction dependency for the slip and normalized road force has been shown in figure 2.2. The slip-based methods collect data during rather low accelerations or decelerations. This can then be used to identify what maximum friction force the tire–road interface can supply, without actually taking the wheels to the verge of skidding, alternatively spinning and thereby cause instability.

The effective radii of the tires will be variable since the normal forces acting on the tires will depend on the acceleration of the vehicle. Unless accounted for, this can introduce errors in the slip calculations.

With knowledge of how the slip curve looks for low road forces it is possible to predict the rest of the curve by fitting a slip shaped function to the data, whether it may be a polynomial or the Pacejka-Bakker Magic Formula (equation 2.3). However, with noisy speed measurements, it may not be suitable to use these methods. Since it seems as the initial slope of the slip curve differs for different surfaces, one can do a least squares fit of a line to the data instead.

An experimentally successful approach [Gus95] is to use a Kalman filter to recursively estimate both the offset and the slope of the slip curve. A Kalman filter was chosen due to its ability to track parameters with different speeds. Due to slow convergence when the slip slope changes abruptly, for instance when driving into a patch of snow on the road, an abrupt change detector is used to adjust the Kalman filter parameters to emphasize speed rather than accuracy. The main advantage with this approach is that the slope and offset are continuously fed out from the filter, whereas when using a least squares fit, a whole sequence of braking or acceleration has to take place first, before the regression can start.

### 3.3.1 Acceleration

During acceleration, assuming two-wheel drive, the slip can be calculated using the non driving wheels for obtaining the velocity of the car.

One approach [YHL99] of measuring the force generated by the road during acceleration is to add engine and transmission output RPM sensors in addition to a throttle position sensor. The output from these can be fed into an observer which uses a vehicle/transmission model to output the friction force.

### 3.3.2 Deceleration

An alternative approach is to calculate slip from deceleration instead. One problem that arises is how the velocity of the vehicle can be obtained when all wheels are significantly slipping due to braking. The solution could be to design an observer which would use additional sensors, for instance an accelerometer, to output the velocity. A first step in a research project could be to simply brake with two wheels and use the others to obtain the speed of the vehicle.

# Chapter 4

# Experimental Setup

## 4.1 The car

The car that was available for experiments was a red Lincoln Towncar from 1990. This is a big car with ABS system and a V8 engine. The car has been used in the AHS project and is therefore equipped with hardware for longitudinal control. There is no lateral control implemented on the car.

### 4.1.1 Brake system

The brake system in the car is constructed as shown in figure 4.1. The brake pedal generates a brake pressure in the master cylinder fluid. Normally, the outputs from the master cylinder is connected directly to the brakes. In a car equipped with ABS system, there are two valves between the master cylinder and the brake. Normally, the build valve is open and the dump valve is closed. When the ABS unit detects that a wheel is close to locking up, it closes the build valve, preventing the pressure in the brake to build up further. The dump valve then opens slightly, which decreases the pressure in the brake, and the wheel will then start rolling again.

The anti-lock function of the brakes is not used in the experiments. The dump valve is always closed, but the build valve can be shut off in order to switch off the brakes on selected wheels.

When driving the car with automated control, a brake actuator moves the piston in the master cylinder, forcing a pressure to build up.

### 4.1.2 Sensors

#### Wheel speed sensors

The four wheel velocities are measured by one sensor per wheel. This is the standard type of sensor used for the ABS system, and it is installed in the car as standard equipment.

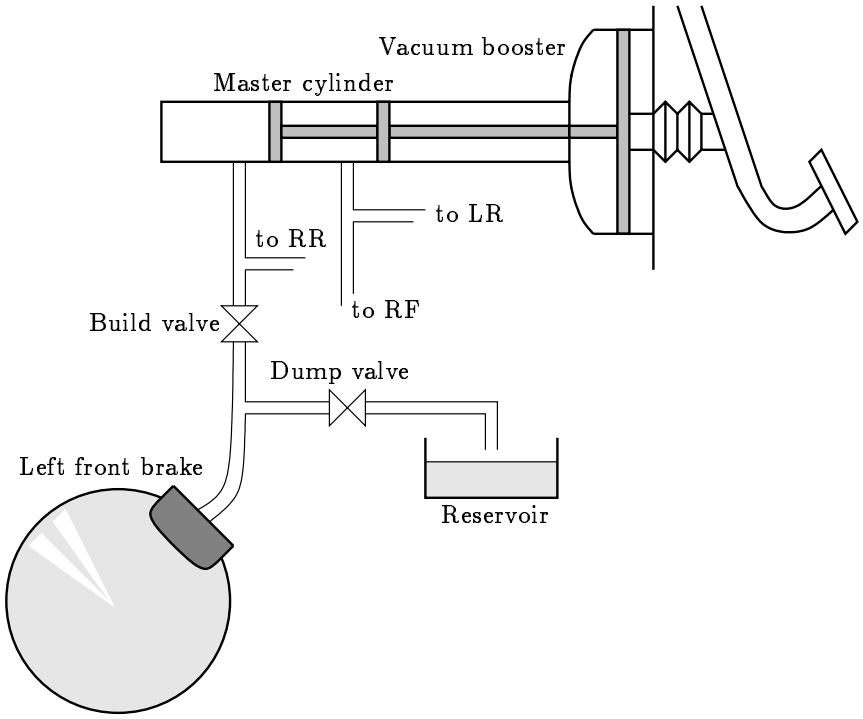


Figure 4.1: Brake system.

The sensor consists of a metal disc with 50 teeth, which is rotating together with the wheel. When the disc rotates, the teeth will affect a magnetic field from a magnet. Depending on if there is a tooth pointing out from the disc, the flux will be different. The variation of flux will induce a voltage in a coil mounted close to the magnet, and this voltage will have a frequency proportional to the speed of the wheel. The period time of this signal is measured for the speed calculations.

### Torque sensor

On the left front wheel a torque sensor is mounted, see figure 4.2. The brake rotor has strain gauges attached to it, so when there is a torque on the brake rotor, the strain gauges will give a signal. Because of that the rear wheels are the driving wheels, there will only be significant torque during braking.

The signal from the torque sensor is proportional to the torque on the wheel except for a voltage offset.

The torque sensor is not a good choice for practical use, because it is too expensive and the way it is implemented on the test car is not suitable for standard production.

Figure 4.2: Torque sensor.

#### Accelerometer

A chassis-mounted accelerometer gives a measurement of the acceleration of the vehicle.

#### Brake pressure gauges

There are pressure gauges mounted to the hydraulic brake system, reading the pressure of the brake fluid at the different brakes.

#### Engine sensors

In addition to the previous sensors, there are also a couple of engine sensors: the engine throttle, manifold pressure, engine speed and the gear ratio. These are, however, not used in this report.

### 4.1.3 Data acquisition

The data is gathered by a computer in the trunk of the car. The computer has a number of I/O ports and runs the QNX operating system. Data is collected with 5 ms sample time.

## 4.2 Test track

The test road at Richmond Field Station is a track used for development of the automatic highways. The track is about 150 m long, and this length is to be used both for acceleration and braking. The track also has a turn in the middle, with approximately 70 m straight road after the turn. This means that to assure only longitudinal forces on the car, all the measurements must be carried out on the straight part of the track.

# Chapter 5

# Chosen Approach

## 5.1 Choice of slip-based method

Choosing from the methods to determine road conditions described in chapter 3, the one that best suits the experimental conditions should be used. The slip approach is chosen, because it gives the opportunity to classify the type of surface without adding any expensive additional sensors.

The idea is based on the assumption that when looking at the slip curve, the slope at the beginning of the curve contains sufficient information to give a value of the maximal friction. This method has been experimentally verified to be able to distinguish between different road conditions [Gus95].

The main work in this project will therefore consist of achieving good measurements, and processing them so that it is as easy as possible to estimate the slope of the slip curve.

## 5.2 Choice between acceleration and deceleration

What type of tests should the work be concentrated on? The fundamental decision that has to be made is whether to only use braking, acceleration or both. Some force excitation in either direction is necessary to achieve sufficient slip.

The project had to be concentrated on one of the approaches; looking at both acceleration and braking would take too much time. The choice fell on just examining braking. This was partly due to that it is easier to estimate the friction force when braking, because of its correspondence to the brake torque. The brake torque can be calculated from the brake pressure, as described in chapter 8. A torque sensor which is installed in the car is used to verify the force estimation.

The disadvantage with using accelerations for force estimation is that many engine and drive train parameters has to be taken into consideration.

# Chapter 6

# Experimental Considerations

Given the experimental environment described in chapter 4, how should the experiments be performed to give the best results?

## 6.1 Need of reference speed

Getting good slip estimates requires good speed measurements. As seen in the slip definition in equation 2.1, the actual velocity of the vehicle is needed. If the car brakes with all four wheels, it is impossible to use one of the speed measurements as the reference speed. All wheels will have slip to some degree. A choice between the different ways to estimate the real vehicle speed is therefore necessary:

**Use a fifth wheel.** This would probably be the best solution during the development stage. With a light extra wheel, a constant normal force can be maintained, and radius changes due to pitching of the car can be avoided. Since the car was not equipped with an extra wheel, this solution could not be used.

**Do not brake with all four wheels.** If not braking with the rear wheels, but just letting them roll free, they will not have any slip caused by friction, and they can be used as speed reference.

**Use a velocity observer.** For the final version of a road classifier, the car has to brake with all four wheels, and an extra wheel is not practical to use either. The correct speed has to be estimated from different measurements. To do this an observer could be used that tries to estimate the correct velocity. The automated highways are also equipped with magnets spread out with a certain spacing in the road. This could also serve as a help for the observer to estimate the correct speed.

Which of these three points should be used in our case? The choice fell on braking with just one pair of wheels, because the car is equipped with a brake system that allows switching off the braking on desired wheels. The fifth wheel was not an alternative to use, and the observer was decided to be taken care of in the future instead.

## 6.2 Choice of wheels used for braking

Which wheels should be braking in the experiments? The decision was to brake with only the front wheels. The front wheels are more important than the rear wheels during braking, because of the increase in normal force on the front axis when the car pitches forward. The rear wheels are here only used as speed reference.

After making the decision not to brake with the rear wheels, another choice that has to be made is whether to brake with one or two front wheels. There are advantages with either choice:

### Advantages with braking with one wheel

- When the vehicle decelerates, it pitches forward. Braking with only one front wheel would give the opportunity to use the other front wheel as a reliable speed reference. Since any changes in the wheel radius would affect both front wheels the same, the radius changes would cancel out each other in the slip calculations.

- The pitching will be smaller for a given tire friction force, because of the lower deceleration when braking with one wheel.

- The friction force for the braking wheel corresponds directly to the force that is decelerating the car.

### Advantages with braking with two wheels

- Since both front wheels brake equally, there will not be any yaw of the car. Since there will not be any lateral forces, there will be no side slip on the tires.

- It is preferred that the tests are carried out under as realistic conditions as possible. Normally, the car brakes with all four wheels, which makes braking with two wheels instead of one wheel the more realistic choice.

- Since the test track was rather short, braking with two wheels would allow us to reach a higher and more realistic speed without compromising security.

The absence of lateral forces when braking with both front wheels seems rather important, and since the tests look more like the real conditions when braking with more wheels, there are more advantages with braking with two wheels than when braking with only one. In most of the tests both front wheels therefore are used for braking.

## 6.3 Road surfaces

The goal of the project is to distinguish between different road surfaces. Since the car is an experimental vehicle, not allowed to drive on public roads, the measurements were restricted to the test track.

The different surfaces that were considered was dry and wet asphalt. Making tests on snow or ice is not possible in the part of California where the test track was located. It also turned out that since it does not rain very often, water had to be poured on the track some times to get a wet road. In these cases, water was just poured on the part where the car was braking. The three road surfaces used it the tests are:

- Dry asphalt
- Wet asphalt, obtained by pouring about 275 liters of water over an area of 120 $m^2$
- Wet asphalt, wet by rain water

## 6.4 Test profiles

### 6.4.1 The need of road force excitation

As described before, there is a need of force excitation to get slip from the wheels. Because the goal is to look at the slope at the beginning of the slip curve, the points should be spread out so that fitting a line to the points can be done with good accuracy. All points should not be placed in the same part of the plot, because the noise will then be very large compared to the real excitation in the force and slip axes. Assigning a straight line to points placed mainly by noise is hard. Considering this, the solution is to have the force values spread out over many places on the force axis.

### 6.4.2 Automatic driving

The test vehicle is equipped with automatic longitudinal control. With this it is possible to tell the car to follow a desired speed profile, which includes acceleration and braking. A typical look of a speed profile with automatic control can be seen in figure 6.1a. The profile includes a ramp acceleration, a part with constant speed, and a braking part also following a velocity

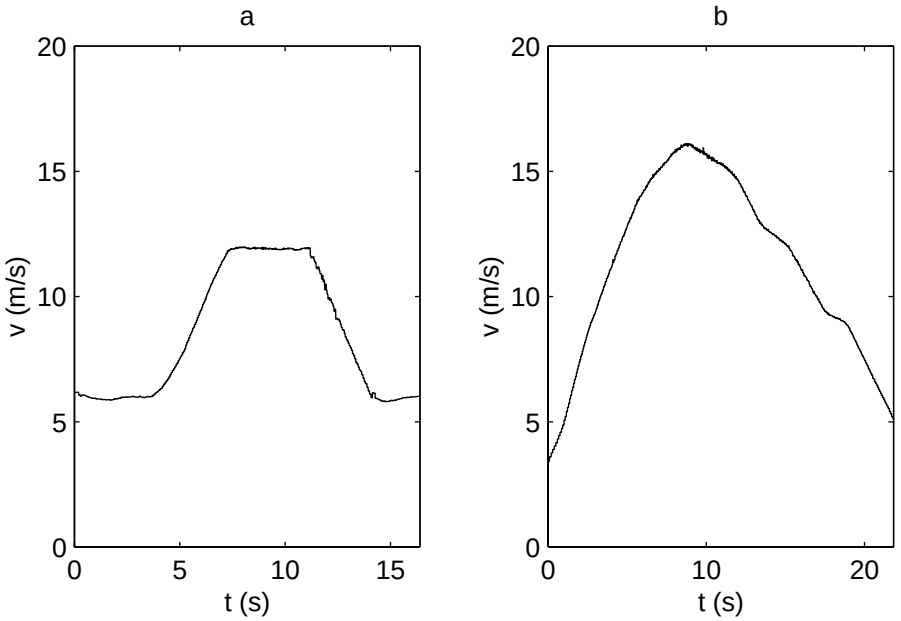


Figure 6.1: Example of speed profiles: a) automatic control, b) cycling with manual control.

ramp. Ramp braking corresponds to constant deceleration, which means a constant force. The points in the slip curve plot will then be concentrated to a certain force value, which will give a bad line fit. This disadvantage with the automatic control tests made that the work is concentrated on tests with manual driving.

Since the goal with the AHS is to have fully automatic control, there could be a contradiction here: should not the tests be under automatic control when the work is part of an automatic control project? In the automatic controlled cars, ramp braking is not the most preferable type of braking, since the comfort of the passengers should also be considered. Therefore, this will not cause a problem in the later stages of development.

### 6.4.3 Manual driving

The advantage with automatic control is that the vehicle can be told to follow the same speed profile for different surfaces. This gives the the opportunity to compare different runs of the same test profile.

When driving with manual control, two totally identical tests cannot be generated. Driving a series of different tests gives good results anyway so manual driving is used in most of the tests. Variation between the tests can be achieved by having different velocities and different pressures on the brake pedal. The type of braking profiles can be separated in two major areas:

**Plain braking.** Here the brakes are applied until the car reaches a slow speed or stops.

**Cyclic braking.** The brake pedal is pushed several times, making the deceleration vary with time. A typical test can be seen in figure 6.1b. Up to 9 s the vehicle accelerates, and the brakes are applied the first time after about 11.5 s.

# Chapter 7

# Slip Estimation

Looking at the slip definition in equation 2.1, the importance of good speed measurements can be noted. Since the difference is taken between two almost identical values, all that is left could be the noise if the measurements are processed in the wrong way.

## 7.1 Choice between speed measurements

### 7.1.1 Wheel speed signals

As described in section 4.1.2, the signal from the speed sensor is generated by electrical induction,

$$\varepsilon = -N\frac{d\phi}{dt}, \tag{7.1}$$

where the flux $\phi$ has a frequency proportional to the speed of the wheel. The formula shows that if the speed is higher, the derivative of the flux will be larger, since the time from a top value to a bottom value of the flux is shorter. The amplitude of the voltage will therefore be larger at a higher speed.

The output from the coil is a periodically varying voltage with an amplitude proportional to the speed of the wheel. The time duration for each pulse is measured with a timing circuit. To prevent noise from the measurements from trigging the timer more than once per pulse, the signal is connected through a hysteresis unit. Since the amplitude for low speed signals is smaller than the amplitude for high speed signals, two different hysteresis bands are used in parallel. The timer measures how long time a half period of the hysteresis output takes, and this result is read as input to the data acquisition board in the computer.

### 7.1.2 The *high* and *divide* signals

Since there are two different hysteresis bands, two different input variables are used in the computer. One is called the *high* signal, and one the *low* signal. The first one uses a larger hysteresis band than the latter. The *low* signal does not give any results for speeds over approximately 6 m/s, so this sensor is not useful for us at all. This signal is mainly used for having good control over the start and stop maneuvers of the Automated Highway System. In this work only speeds over 5 m/s are considered.

When the speed is even higher, the time for each tooth pulse gets shorter, and the accuracy of the measurements gets worse. In the timer circuit there also is a circuit that divides the pulse frequency with a factor of ten. Since the time period in to the timer will consist of ten tooth pulses, the time will be averaged and the results probably better at higher speeds. This speed measurement is called the *divide* signal.

### 7.1.3 Improving the *divide* signal

The *divide* signal is updated every ten teeth on the wheel, which means five times per wheel rotation. One problem is that all four wheels update the data values independently. If one wheel is a little bit smaller, or if the road turns, there will be a difference in time between the new values. During the time between two sample values, the signal keeps the old value. This makes it hard to compare the speed from two different wheels, since the two speed values are based on two different time intervals.

The shape of the *divide* signal is stair-like, since its update frequency is smaller than the sampling frequency. Only the first value in a row of consecutive samples gives new information about the speed of the wheel. The other following samples based on the same measurement should be discarded.

Each new value of the *divide* signal comes after the period it is averaged from. To get the sample time right, this sample should be moved to an earlier time so that it is in the middle of the corresponding time interval. It is possible to calculate the length of this time interval in number of samples. If the car is driving at speed $v$, the period time for one wheel rotation is

$$T_w = \frac{1}{f} = \frac{1}{\frac{\omega}{2\pi}} = \frac{2\pi}{\frac{v}{r}} = \frac{2\pi r}{v}. \tag{7.2}$$

Since there are 50 teeth per wheel and the *divide* signal is made up of 10 teeth, the number of samples per value of the *divide* signal is

$$N = 10\frac{T_w/50}{T_s} = \frac{T_w}{5T_s} = \frac{2\pi r}{5T_s v}, \tag{7.3}$$

where $T_s$ is the sampling interval.

Moving the point half this number of samples earlier in time and connecting the points with straight lines gives an approximation that better

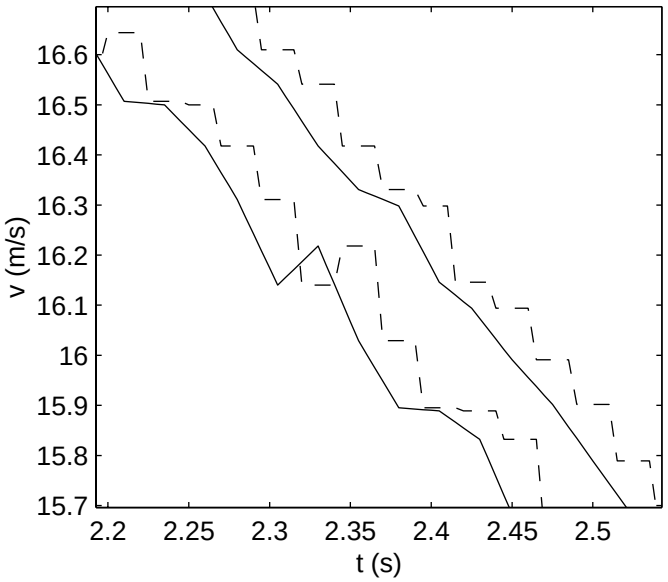


Figure 7.1: Modifying the *divide* wheel speed signal. The unmodified signals dashed and the modified signals solid. The upper two lines are the right wheel and the lower two are the left wheel.

corresponds to the actual speed, without time delays. Look at the solid lines in figure 7.1.

### 7.1.4 Comparing the accuracy of different measurements

After making these adjustments to the *divide* signal, which signal to use is a question to be answered. Perhaps both of them could be used in some way.

When plotting the both signals together, the *high* signal seems to have a higher value. This can be explained by that the timer can only count whole time intervals. Since many small intervals can add up into one whole clock tick, the *divide* signal will in average measure a longer time, which will give a lower, but more correct, speed. See figure 7.2 where the shaded areas are not included in the timer measurements. Since the timer only measures the time of the high part of the pulses, the speed measurements will be depending on the duty cycle of the pulse signal. The *divide* measurement is averaged from both high and low values of the pulses, and this explains also why there is a difference between the measurements. The conclusion is that it is necessary to use the same type of measurement the whole time, since switching between the two types could introduce problems caused by offsets.

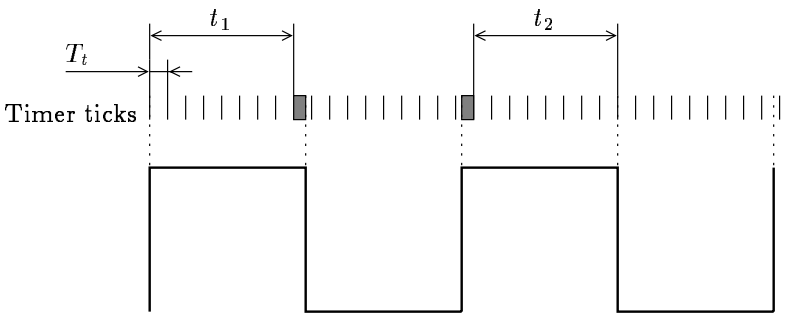


Figure 7.2: Estimating the frequency by measuring the half-period time. Note the shaded areas which are missed due to the frequency of the timer tick.

### 7.1.5 Choice of which measurements to use

The advantage with using the *divide* signal is that it has a smaller level of noise. It is also built up by several consecutive teeth, a method which gives a rather good averaged value. The disadvantage is that the signals for different wheels are asynchronous to another, and have a certain time lag. This could be corrected, as shown above.

The reason to use the *high* signal is that it is updated every sample interval. All teeth are however not measured, since the tooth frequency is higher than the sampling frequency. This makes it impossible to find ten consecutive teeth to average over.

**Example 7.1.1** *Assume that the vehicle speed is* $v = 15m/s$. *The angular velocity of a wheel will then be* $\omega = \frac{v}{r_w}$, *which corresponds to a pulse frequency of* $f = 50\frac{\omega}{2\pi r_w} = \frac{50 \cdot 15}{2\pi \cdot 0.33}\,\mathrm{Hz} = 362\,\mathrm{Hz}$, *which is faster than the sampling frequency of* $200\,\mathrm{Hz}$. *Therefore it is impossible to get the time period of each tooth to make an averaging over consecutive samples.* □

The choice fell on using the *divide* signal as the source of our speed values. It is more important to have a low noise value than to have a lot of different samples. The classifier is not dependent of a high sampling frequency as a control algorithm is. The best way to use the existing car sensors would probably have been to modify the averaging algorithm in the hardware and timer board, so that all wheel signals always were averaged over the same time interval.

## 7.2 Noise characteristics

How could the noise in the speed signals be reduced? Especially in the *high* signal, there is significantly high noise. Using some kind of frequency filtering

is a natural approach to start with.

Looking at the frequency for the different wheels, it can be noted that the noise spectrum does not have the same look for all tests. The different wheels also show differences in noise characteristics. The two front wheels typically have noise that has its highest values in the region below 40 Hz, whereas the rear wheels do not show this low frequency concentration. Instead, sometimes there exists a higher noise frequency for the rear wheels.

One possible explanation of the noise could be that it is caused by irregularities in the wheel radii. This type of noise would have a frequency at the same frequency as the wheel angular velocity, or overtones of that. Such kind of frequencies could not be concluded to be especially visible, so other types of noise are also present.

There are probably other vibrations and oscillations in the car, causing noise in the wheel speed sensors. The low frequency components for the front wheels, up to $40\,\mathrm{Hz} = 2400\,\mathrm{rpm}$, can for example be caused by engine vibrations.

Is it then possible to filter the speed signals to get rid of the noise? Using a low pass filter gave the results that all high frequency components were removed, but low frequency oscillations were still visible, both in the filtered wheel speed signals and in the slip values. Using a low pass filter would also require a quite high order filter, and the long impulse response of such a filter gives a very smoothed out look of the slip data.

The conclusion is that a high order low pass filter is not useful for filtering. Since fitting a line through data points can be done even if the points are somewhat spread out, but not as easy if the points follow some low frequency oscillation, low pass filtering could only be used to take away some of the highest noise frequencies.

# Chapter 8

# Road Force Estimation

The slip curves consist of both a slip axis as well as a normalized friction force axis. It is therefore essential to have reliable information about the friction force that is acting on the road during a braking sequence.

## 8.1 Using acceleration

Assuming no aerodynamic drag or rolling resistance, the resulting force on the car during deceleration will only consist of the force acting on the braking wheels, according to

$$\sum_{\substack{\text{braking}\\ \text{wheels}}} F = ma. \tag{8.1}$$

The acceleration can be acquired by differentiating the wheel speed measurements, however this method does not work particularly well when the speed measurements are quite noisy in the first place. Another way to get the acceleration would be to use an accelerometer, which has the drawback that it requires an extra sensor.

## 8.2 Using brake pressure

Any car equipped with hardware for automated control would need brake pressure sensors, so using the brake pressure sensors for obtaining the road force would not introduce any additional costs. The brake pressure, $p_b$, is related to the brake torque, $\tau_b$, according to

$$\tau_b = -K_b p_b \operatorname{sign}(\omega). \tag{8.2}$$

However, this simple model is not always valid. The brake pads are held back from the brake disc with a spring. Thus, it takes a certain force to move the brake pads the distance to the disc surface. This means that there is an offset in the term above.

The parameter $K_b$, which describes the scaling between the pressure and the torque, is varying. This is caused by for example differences in temperature and how worn out the brake pads are. To get a good estimate of the brake torque, $K_b$ has to be adapted. An algorithm is being developed by members of the research group at PATH to adaptively estimate $K_b$ without the need of any extra sensors. With this in mind, we used the measurements of the torque sensor to get a value of $K_b$ by dividing the brake torque with the brake pressure. One of the goals of this project was to minimize the use of non-standard sensors, such as for instance the torque sensor. Although, bearing in mind that the adaptive algorithm was being developed, the torque sensor would only be used during the development stage of the project and could be replaced by the adaptive algorithm further on.

The brake torque is related to the road force by

$$J\dot{\omega} = \tau_b - F_{road}r, \tag{8.3}$$

were $r$ is the radius of the wheel. Once the road force, $F_{road}$, is calculated, it needs to be normalized by the normal force, $N$, acting on the actual wheel. The normalized road force, $\mu$, will then become

$$\mu = \frac{F_{road}}{N}. \tag{8.4}$$

Since the normal force is not equal on all wheels during deceleration, the force acting on the front wheels will be larger than the force acting on the rear wheels. The normal force on the front wheel axle is given by [Gil92]

$$N_{Front} = \frac{\frac{mg}{2}L_R - \frac{ah}{g}}{L} \tag{8.5}$$

where $m$ is the mass of the car, $g$ the gravity constant, $a$ the acceleration, $h$ the distance from center of gravity to the ground, $L$ the distance between the two wheel axles and $L_R$ is the distance between center of gravity and the rear wheel axle.

# Chapter 9

# Classification Part I

This chapter consists of the different methods used for classifying the first set of test runs. As our methods became more sophisticated, new tests were also acquired, described in Chapter 13.

## 9.1 Initial tests

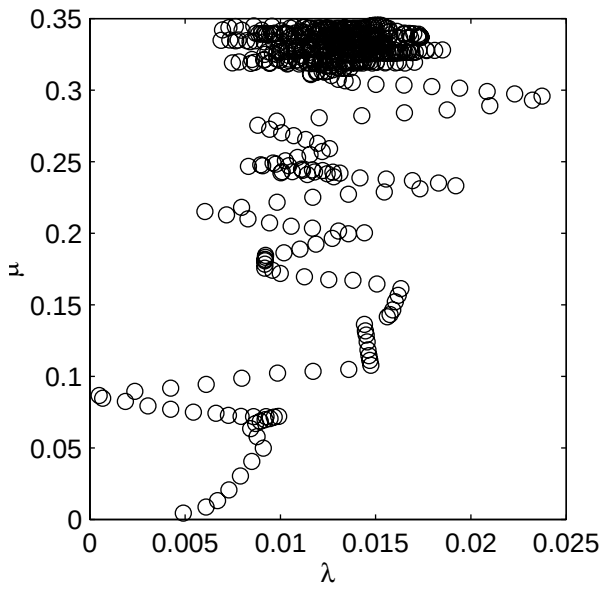


Figure 9.1: Slip curve for a typical test run

The tests mainly consisted of manual driving of the car and plain braking. Due to the limitations in weather in California our tests at this stage consist only of driving on dry and wet pavement, where the wet pavement was

acquired by pouring large amounts of water on the track.

Since the wheel-speed measurements have a lot of uncertainly for speeds below 5 m/s, those parts were cut off from the raw data. Anything else besides strictly braking was also removed from the data.

A typical test run with the car would generate raw slip-curve data according to figure 9.1. The offset in the slip axis is due to radii differences between the front and rear wheels. Even if it is not very obvious in the mentioned figure, it can be noted that the slip slope seemed to be flatter for low $\mu$ values, and steeper for high $\mu$ values.

## 9.2 Linear curve fitting

### 9.2.1 Least squares fitting of a line

The simplest way to classify the different surfaces would be to do a least squares fit to the data. Such a classification is shown in figure 9.2. It does not seem possible to draw any conclusions about the road surface by looking

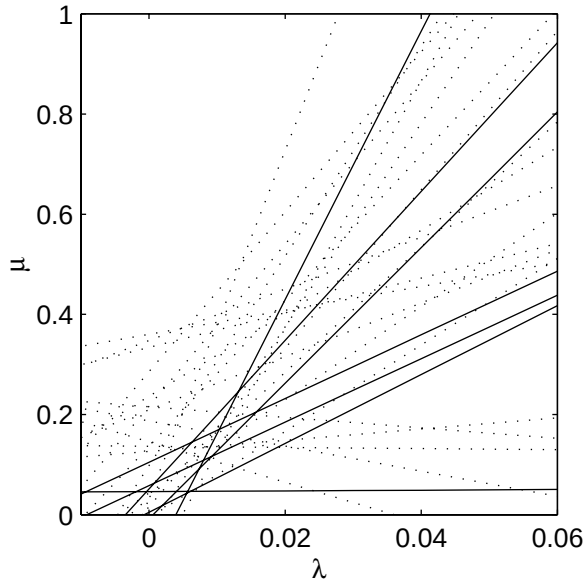


Figure 9.2: Least squares fit for slip curves for wet (solid) and dry pavement (dotted).

at the slope of the least squares fits. The line fits to the data can have the completely wrong slope, making this first approach not a very suitable one.

When braking with a rather constant brake torque, as done in these tests, the slip data will correspond to a certain value of normalized friction force. In theory there would be just a point in the slip curve, but since the speed

measurements are rather noisy, the slip data are spread out. Since the noisy slip data is not equally spread out along the $\mu$ axis, there will be an uneven weighting of the data. In an arbitrary test run, a majority of the slip data will correspond to an interval covering only a small percentage of the $\mu$ axis. Since the least squares method minimizes the squared distance from the line fit to the data, this will cause the fit to be poor.

### 9.2.2 Averaging over the slip axis

The friction force data is much less noisy than the slip data, i.e. for a small interval of the friction force there is a large spread of slip values.

The $\mu$ axis is divided into several bins, where the slip values are averaged for all points in each bin. This leads to that for a certain test run, there will only be one value of slip for each bin in the force axis. By doing a least squares fit to this data, all points along the force axis will be equally weighted, as opposed to in the previous methods. Several wet and dry tests averaged according to the procedure described are shown in figure 9.3. Even if the slopes of the slip curves sometimes obviously are wrong, it seems to

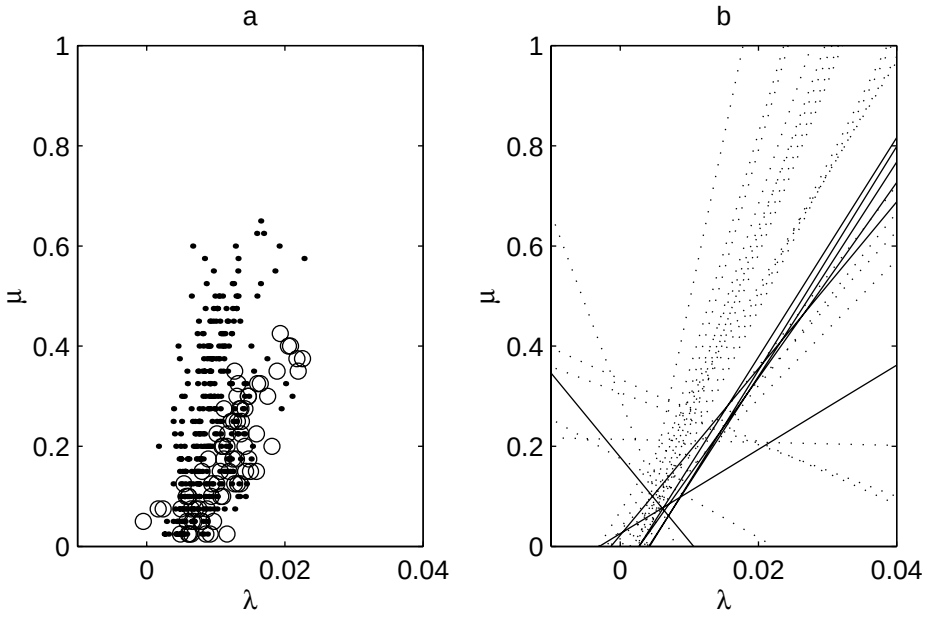


Figure 9.3: a) Data from several test runs using the averaging method for wet (circles) and dry pavement (dots). b) Least squares fits to the data in a). Wet corresponds to solid lines, dry to dotted lines.

be possible to differentiate between the dry and wet pavement based on the slope of the least squares fit.

### 9.2.3 Calculating the offset before the slope

A method that supposedly would solve the problem of getting strange slopes for the fits was also investigated. The averaging method described in the previous section is still used. The idea is to first calculate the offset in the slip during coasting, and then during braking, subtract the offset from the slip. The least squares fit would be forced to go through the origin, hence only estimate the slope. As seen in figure 9.4 the result is still not very

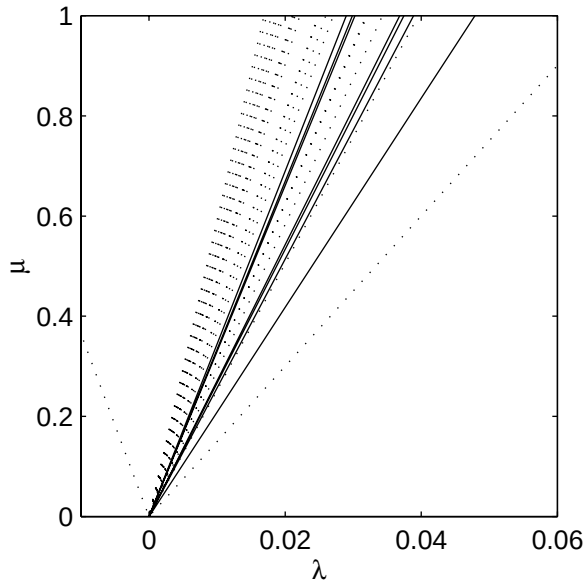


Figure 9.4: Least squares fit for wet (solid) and dry pavement (dotted), where the slip offset first was calculated and then taken into account.

satisfying. The reason for this is mainly because of the loss of information during the two steps. A better approach would be to calculate the slip and offset at the same time, as done in Chapter 11. It seemed as if the offset calculations introduced some uncertainty, especially for the tests that did not have sufficient time of coasting before braking.

## 9.3 Curve fitting to functions capturing the slip curve essentials

Instead of fitting a line to the $\lambda$–$\mu$ data, a function that captures the shape of a slip curve could be used instead. The parameters of the function would then be fitted to the data using the least squares method. The idea would be to use the parameters of the function to distinguish between different

road surfaces. Naturally this implies that there is a similarity between the parameters for a certain road surface.

### 9.3.1 Using the Pacejka–Bakker tire model

The Pacejka–Bakker Magic Formula, (equation 2.3), is an empirical tire model that can be used for generating slip curves. Since the Magic Formula is nonlinear, an approximation,

$$\theta_1 \cdot e^{-\theta_2 \lambda} \cdot \lambda^{(\theta_3 \lambda + \theta_4)}, \tag{9.1}$$

was used instead. After taking the logarithm of equation 9.1 we end up with a function that is linear,

$$\ln \theta_1 - \theta_2 \lambda + (\theta_3 \lambda + \theta_4) \ln \lambda. \tag{9.2}$$

When this method was evaluated, the curve fits followed the data quite well in the beginning, but beyond the area from which we had samples, the curve fits went either to infinity or zero. However, it seemed to be no similarity for the parameters for the same surface. Hence, this method was not successful in classifying different road surfaces.

### 9.3.2 Using a polynomial

Since the previous method might have gone wrong because of the complexity of the Magic Formula, a simpler approach was investigated. A polynomial,

$$y = k \frac{s}{ax^2 + bx + 1}, \tag{9.3}$$

which captures the behavior of the slip curves with appropriate values of the parameters, $k$, $a$ and $b$, was used.

The result from this was similar to the results when using the Magic Formula. It was not possible to use the parameters to distinguish between road surfaces.

# Chapter 10

# Simulation Model

The experiments in chapter 9 showed that there was a chance to distinguish between different road surfaces by looking at the slope at the beginning of the slip curves. To further improve the estimation and classification methods, it would be nice to have a simulation model that could generate data for the algorithms. The goal is to make the simulation model produce the same type of output as the measurements from the car.

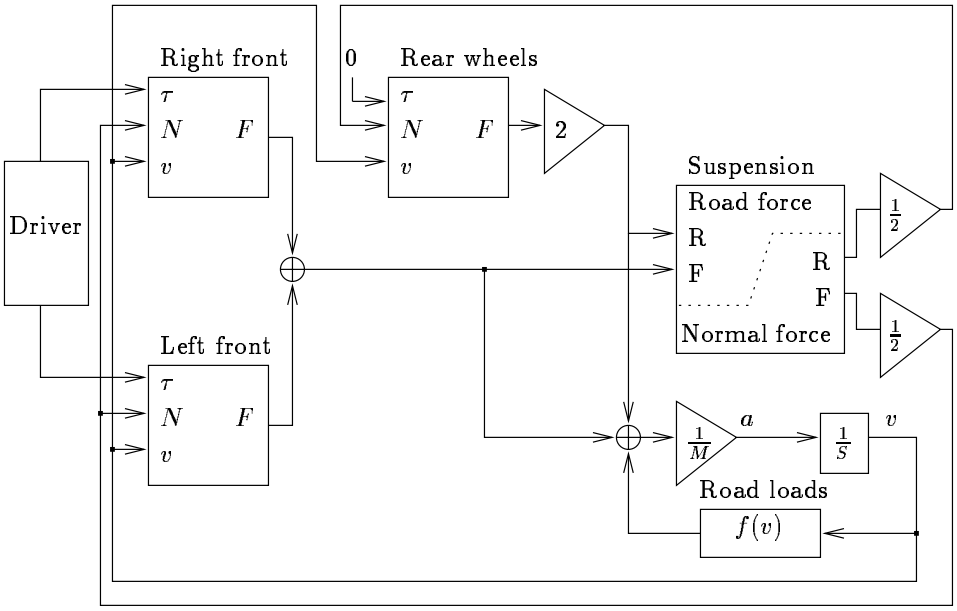


Figure 10.1: Top diagram of the simulation model.

A simulation model was built in Simulink for use in the further work. The model simulates a car driving on a long straight road, since the experimental

work only included braking on the straight part of the track. The model does not include any lateral forces at all, and can be considered as a half-car model.

## 10.1 Top level model

Normally, a half-car simulation model has two wheels, but this model works with two front wheels and one rear wheel. This is because it should be able to simulate braking maneuvers with just one of the front wheels. The lateral forces generated in these operations are not modeled at all, but the idea was to still keep the opportunity to see how the free-rolling front wheel is affected when the other wheel is braking. There are changes in normal force during deceleration, which could affect the radii of the front wheels. A block diagram of the model is shown in figure 10.1. There are three identical objects, two representing the front wheels and one representing the rear axle. The suspension block models the pitching of the car and distribution of normal forces which is described later. The $F$ signals coming out from the three wheel blocks are the road forces, which are added together to give the acceleration of the vehicle. There is also an opportunity to include rolling resistance and drag force as a function of velocity in the Road loads block, see section 10.4.

## 10.2 Wheel modeling

The three identical wheel objects consist of the dynamics for the wheel according to figure 2.4. The Simulink block for the wheel is built up as shown in figure 10.2. The block with the slip formula calculates the slip value,

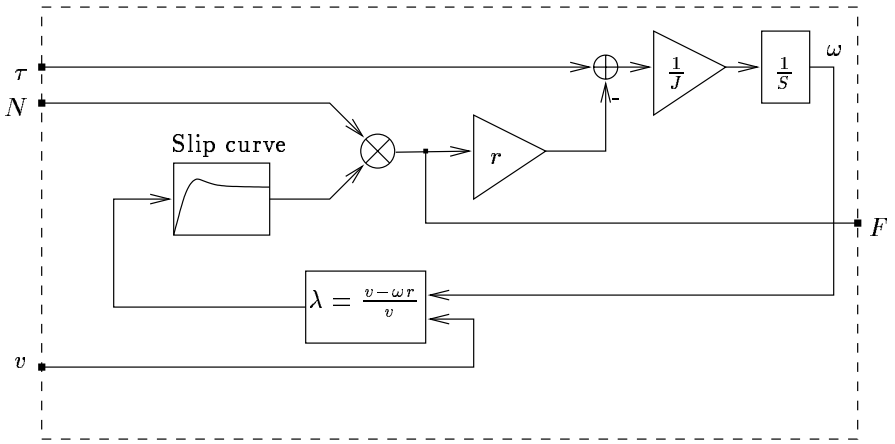


Figure 10.2: Simulation block of one wheel.

based on the angular velocity of the wheel and the velocity of the vehicle, a signal coming from the top level of the model.

The block marked "Slip curve" is a predefined slip curve used in the simulation. The slip curve is selected depending on the type of surface the test should simulate.

## 10.3 Suspension modeling

To include the pitching behavior of the car, a model of the car suspension was made, see figure 10.3. The approximations $\sin\theta \approx \theta$ and $\cos\theta \approx 1$ has been made both in the picture and in the following equations. This model has two degrees of freedom. One is $\theta$ for the pitch of the car, positive when the front is higher. The other is $z$, which together with the constant $h$ describes the distance from the center of gravity, CG, to the ground.

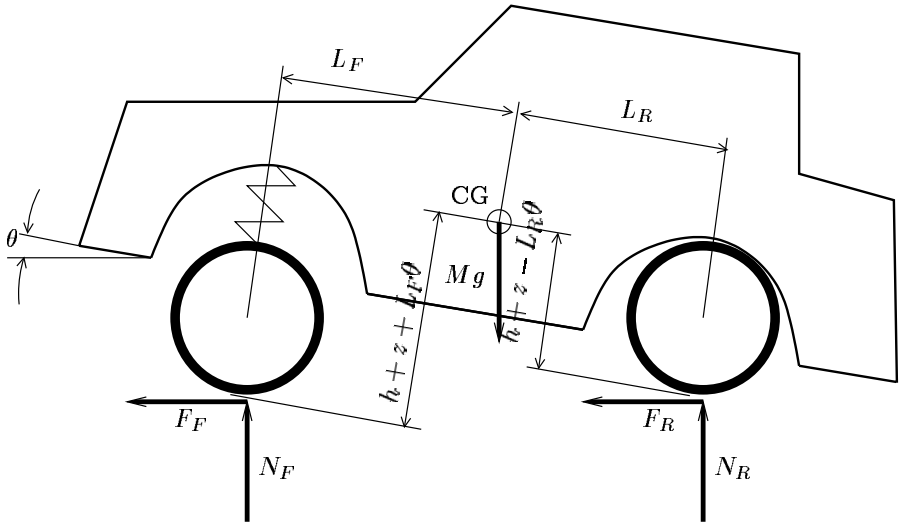


Figure 10.3: Suspension model.

According to figure 10.3, the equations of motion can be written as

$$\ddot{\theta} = \frac{1}{J_c}\left(F_F(h+z+L_F\theta) + F_R(h+z-L_R\theta) + N_F L_F - N_R L_R\right) \quad (10.1)$$

$$\ddot{z} = \frac{1}{M}\left(N_F + N_R\right) - g, \quad (10.2)$$

where $M$ is the mass of the car, $J_C$ is the pitch moment of inertia, and $g$ the gravity constant.

## 10.4 Decelerating forces

Road force generated by the brake torques is not the only force decelerating the car. Also other forces can be modeled.

### 10.4.1 Rolling resistance

According to Gillespie [Gil92], the total rolling resistance $R_x$ for the tires can be modeled as

$$R_x = (0.0041 + 0.000041 v_{\text{mph}}) C_h W = (0.0041 + 9.225 \cdot 10^{-5} v_{\text{m/s}}) C_h W, \tag{10.3}$$

where $W$ is the weight of the vehicle and $C_h$ is the road surface coefficient, $C_h$ =1–1.5 depending on road surface.

### 10.4.2 Drag force

The drag force can be calculated [Gil92] as

$$D_A = \frac{1}{2} \rho v^2 C_D A, \tag{10.4}$$

where $C_D$=0.3–0.6 is the aerodynamic drag coefficient, $\rho \approx 1.225 \frac{\text{kg}}{\text{m}^3}$ the density of the air and $A$ the frontal area of the car.

### 10.4.3 Implementing a simulation model

These two forces are modeled in the Road loads block in figure 10.1, together with some extra force corresponding to engine and drive train braking force. The value of this force is determined by looking at measurements from the vehicle and estimating the braking force.

## 10.5 Running the simulations

The purpose with the simulations is not to give exactly the same outputs as the experimental measurements. This is too hard to achieve, because then all physical constants in the model has to be known exactly. The goal is to make the simulation model generate data having the same over-all properties as the experiments.

At startup the simulation model is given some initial values, such as a specified constant velocity. Equilibrium values of $\theta$ and $z$ are also calculated, making sure there are no initial oscillations before any forces are applied.

### 10.5.1 Braking input

What will affect the result of the simulation is what brake torque the driver block in figure 10.1 gives. To give as realistic look as possible of the speed profile, a real measured sequence of brake pressure samples from an experimental run is used to generate the brake torque. This makes the output of the simulation look very much like the output from the test vehicle. The other alternative would have been to tell the simulation to follow a predefined speed profile, but since manual control is used in the real test runs, the same input was wanted for the simulation.

### 10.5.2 Simulation of different surfaces

As mentioned in the description of the wheel model, different surfaces are simulated using different $\lambda$–$\mu$ characteristics in the wheel block.

If the simulation will include hard braking, a more complete slip curve with a peak has to be used. Since the slip and friction forces should be kept at low values in the tests and the braking is not close to skidding, it is possible to use a linear slip curve without a peak value. This is done by multiplying the normalized friction force with a slope constant. When simulating different road surfaces, different constants are used.

The experiments also showed an offset in the slip curves. In the simulation model, this is generated by varying the ratio between the front and rear wheel radii. If the front wheels are made slightly larger than the rear wheels, they will rotate slower and give the impression of that there is slip even during normal driving.

# Chapter 11

# Recursive Slip Slope Estimation

The way the slip slope has been estimated previously in this report required that the brakes were applied first and then the slip slope could be calculated afterwards using the collected slip data. It would be more realistic if the slip slope could be continuously fed out from a filter during braking. The method, originally proposed by Gustafsson [Gus95], used in this chapter can recursively calculate the offset and the slip slope simultaneously using a Kalman filter. The approach is experimentally verified by Gustafsson to distinguish between dry, icy and snowy roads.

## 11.1 Model

As mentioned in section 2.1.4 the slip is not zero when the friction force is zero. This offset is slowly time varying compared to the slip slope and not correlated with the friction for the tire–road interface. The relationship between the normalized friction force and the slip is denoted by

$$\mu = k(\lambda - \delta) \tag{11.1}$$

where $k$ is the slip slope and $\delta$ the offset. The goal is to produce estimates of both $k$ and $\delta$ simultaneously. Rewriting equation 11.1 as

$$\lambda = \mu\frac{1}{k} + \delta, \tag{11.2}$$

results in getting an expression which gives us an easier filtering problem. This is since $k\delta$ varies much faster than $\delta$. Naturally it is easier to track parameters which are slowly changing than the other way around.

The state space model used for the linear regression is an extension of equation 11.2 according to

$$x(t+1) \quad = \quad x(t) + v(t)$$

$$y(t) = C(t)x(t) + e(t) \tag{11.3}$$

where the state vector is defined as

$$x = \begin{pmatrix} \frac{1}{k(t)} \\ \delta(t) \end{pmatrix}. \tag{11.4}$$

The measurement is the slip and therefore, according to equation 11.2, $C$ becomes

$$C(t) = \begin{pmatrix} \mu(t) & 1 \end{pmatrix}. \tag{11.5}$$

Note how the model assumes that the slip slope and offset do not change over time except for the addition of the process noise $v$, i.e. the model varies like a random walk. Both $v$ and $e$ are considered to be independent random white noise stochastic processes.

## 11.2 The Kalman filter

### 11.2.1 The general case

Given the discrete time system

$$\begin{aligned} x(t+1) &= \Phi x(t) + \Gamma u(t) + v(t) \\ y(t) &= Cx(t) + e(t), \end{aligned} \tag{11.6}$$

the Kalman filter produces the optimal, in the minimum variance sense, estimates to the state vector. The Kalman filter uses measurements up to time $t$ to estimate the states at time $t$. Assuming that the cross correlation between the process noise and measurement noise is zero, which is a good assumption in most applications, the filter is given by the following equations [ÅW97]:

$$\hat{x}(t \mid t) = \hat{x}(t \mid t-1) + K_f(t)(y(t) - C\hat{x}(t \mid t-1)) \tag{11.7}$$

$$\begin{aligned} \hat{x}(t+1 \mid t) &= \Phi\hat{x}(t \mid t) + \Gamma u(t) \\ &= \Phi\hat{x}(t \mid t-1) + \Gamma u(t) \\ &\quad + K(t)(y(t) - C\hat{x}(t \mid t-1)) \end{aligned} \tag{11.8}$$

where the Kalman gain and the Riccati equation are given by

$$K_f(t) = P(t \mid t-1)C^T(CP(t \mid t-1)C^T + R_2)^{-1} \tag{11.9}$$

$$K(t) = \Phi K_f(t) \tag{11.10}$$

$$\begin{aligned} P(t+1 \mid t) &= \Phi P(t \mid t-1)\Phi^T + R_1 \\ &\quad - K(t)(CP(t \mid t-1)C^T + R_2)K(t)^T \end{aligned} \tag{11.11}$$

$$P(0 \mid -1) = R_0 \tag{11.12}$$

where $R_1$ and $R_2$ are defined as the covariance matrices for the process noise, $v$, and the measurement noise, $e$, respectively. $R_0$ is denoted the variance of the initial value of the states, i.e. $R_0 = \mathrm{Var}\{x(0)\}$. Note that the matrix $R_2 + CP(t \mid t-1)C^T$ must be positive definite for the Kalman filter to provide the correct estimates.

### 11.2.2 The recursive slip slope estimator

The equations for the Kalman filter can be simplified when they are being used for estimating the state vector of the recursive slip slope estimator. The cross correlation between the process noise and the measurement noise is assumed to be zero. $\Phi$ is equal to the identity matrix and there is no input, $u$, in our system. This results in that $K = K_f$ and $\hat{x}(t+1 \mid t) = \hat{x}(t \mid t)$. The simplified equations for the Kalman filter turns out to be:

$$\begin{aligned}
\hat{x}(t \mid t) &= \hat{x}(t-1 \mid t-1) \\
&\quad + K(t)(y(t) - C(t)\hat{x}(t-1 \mid t-1)) && (11.13) \\
K(t) &= P(t \mid t-1)C(t)^T \\
&\quad \times (C(t)P(t \mid t-1)C(t)^T + R_2)^{-1} && (11.14) \\
P(t+1 \mid t) &= P(t \mid t-1) + R_1 \\
&\quad - K(t)(C(t)P(t \mid t-1)C(t)^T + R_2)K(t)^T && (11.15) \\
P(0 \mid -1) &= R_0 && (11.16)
\end{aligned}$$

There was a trade off between fast convergence of the Kalman filter and good accuracy. A small value for the diagonal elements of $R_1$ corresponds to accurate values of the slip slope and offset, but also slow tracking capabilities, and vice versa. Since the slip slope was more rapidly changing than the offset, it was important that the filter would be able to track the fast changes in the slip slope, whereas it would weight accuracy more heavily compared to speed for the offset. This was achieved by choosing the element in $R_1$ corresponding to the slip slope to be large compared to the one referring to the offset, which would be relatively small. The covariance matrices were manually tuned in this fashion to get the best possible performance of the filter.

When selecting the different parameters, the simulation model was used to evaluate the filter. The simulation model generated certain slip data with known slip slope, and the Kalman filter's estimation of the slip slope was compared to the known one. Slip curves that suddenly changed slope were also generated by the simulation, in order to see how the tuning of the filter would affect its tracking capabilities.

## 11.3 Decision variable

As mentioned before, the Kalman filter outputs a continuous flow of slip slopes in real time. In order to classify our different test runs, each of those needs to be assigned a decision variable. Since the filter generates many values of slip slope during the course of a test run, one approach would be to pick one of these slopes. The decision variable is chosen to be the value of the slip slope slightly below the maximum friction force.

Once the friction force has reached its peak, the slip corresponding to that value tends to be quite noisy. This would make the slip slope for maximum normalized road force a bad choice of decision variable. Accordingly, choosing the slope slightly below the maximum friction force seems to be a good choice since we then capture the information generated by the Kalman filter, and the force has not yet saturated.

Another approach could be to divide the $\mu$ axis into several bins, and then average the slip slopes corresponding to the actual $\mu$ values and put the result into the bins. This is the same principle as used to average the slip for the slip curves, but the difference is that the slip slopes now are estimated by the Kalman filter. The slip slopes corresponding to the different bins can then be averaged, resulting in a single decision variable for each test run. This method was examined, but was not found to produce equally good results as the previous method mentioned.

## 11.4 Differences to previous work

When driving on a dry road into a patch of ice, the slip slope will go from a high to a low value almost instantly. The Kalman filter will be too slow to track the sudden change of slip slope. In order to be able to detect the sudden changes in road conditions, Gustafsson used an abrupt change detector which would change the covariance matrices for the Kalman filter to weight speed higher than accuracy when the slip slope changed drastically. We did not implement the abrupt change detector due to difficulties setting up two different road surfaces on the rather short track available for tests.

Instead of using the continuous stream of slip slopes that the filter outputs, we used one value as decision variable. Once again, since the track was quite short, it was not possible to take tests that lasted for very long. This made it possible to assume that the slip slope was constant during the deceleration, resulting in one decision variable.

Gustafsson used acceleration to examine slip, when deceleration was used in our case. The test surfaces consisted of snow and ice in addition to wet and dry asphalt. He could not distinguish between wet and dry asphalt, except for one extremely wet road.

# Chapter 12

# Elastic Wheel Observer

In the slip plots in chapter 9, it was noted that the slope of the slip curve was smaller in the beginning, with smaller $\mu$ values, than in the end. When the brakes are released, the slip values decrease much in the beginning, and have a smaller slope in the top of the slip curve. When looking at a cycling test, where the brakes are applied and released several times, the plot has a circular look, that can be seen in figure 12.1.

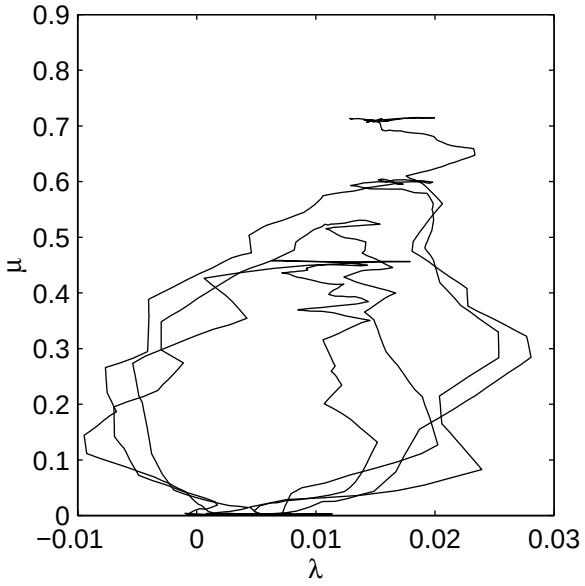


Figure 12.1: Example of a test generating a cycling look of the slip curve.

Since the goal is to estimate the slope of the slip curves, a straight line should be fitted through the slip curve plot. If the figure just contains circles rather than points ordered as a straight line, assigning a correct line will be very difficult to do.

## 12.1 Modeling the behavior

The circular look of the plot must be removed somehow. To do this, a model that includes the look should be developed.

### 12.1.1 Function of the vehicle speed

The idea that the speed of the vehicle explains the differences in slope can be discarded since the cycling tests, where the brake torque is applied several times and at different velocities have the same circular look for each brake period.

### 12.1.2 Change in tire radius

A possible reason is that the radius of the wheel changes during braking. When the brakes are applied, slip will build up due to the road force. When the car then pitches forward, the tires will be compressed to a smaller radius. This makes them roll faster and the increase of slip will not be as high as it was just after the brakes were applied. When the brakes then are released, the wheel will start to roll faster again, but will slow down a bit when the car pitches back, making the wheel radius increase again.

This model has not been examined further, since the following described model seemed to work well.

### 12.1.3 Elasticity of the wheel

An idea is that the wheel elasticity gives the look of the curve. Assume that the tire and the rim are connected together by some elastic binding. When the brakes first are applied, the rim which is connected to the brake disc will start to slow down first, before the tire reacts. This is illustrated in figure 12.2a-c. Wheel a in the figure is a wheel during free rolling. In figure

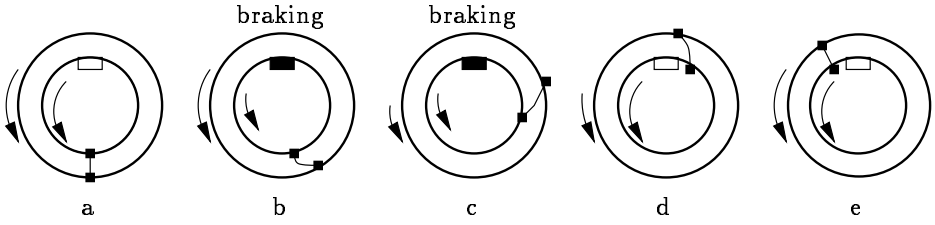


Figure 12.2: A braking maneuver with an elastic wheel.

b the brake is applied. This makes the inner rim slow down but the tire does not react immediately. There will be an increasing angular difference between the tire and the rim. This difference will reach a steady value which

is shown in figure c, where the tire and rim once again rotate with the same speed.

When the brake is released, the rim will notice this change in torque before the tire. Therefore, the rim will rotate faster compared to the tire, figure d, making the angular difference decrease. Finally, the case in figure e is achieved, which is the same as in figure a, with no difference in angle or speed between the tire and rim.

A model of the wheel can now be designed. Assuming that the tire and the rim are two solid parts, connected together with a spring and a damper, the model in figure 12.3 can be drawn. The force between the two parts is

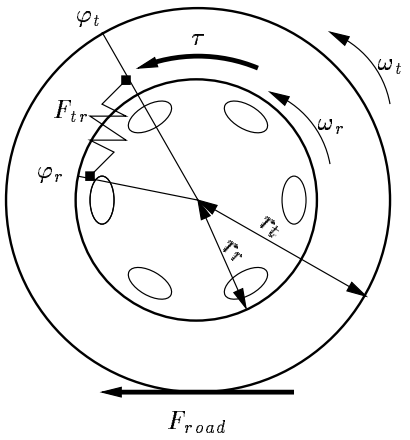


Figure 12.3: Model of the elastic wheel.

assumed to have one part proportional to the difference in angles between the tire and rim, and one part proportional to the derivative of this difference,

$$F_{tr} = K'_{tr}(\varphi_r - \varphi_t) + C'_{tr}(\omega_r - \omega_t). \tag{12.1}$$

This force generates together with the brake torque and road force torques on the two wheel parts,

$$J_r\dot{\omega}_r = \tau - F_{tr}r_r \tag{12.2}$$

and

$$J_t\dot{\omega}_t = F_{tr}r_r - F_{road}r_t. \tag{12.3}$$

To simplify the expression, the rim radius $r_r$ can be included in the damper and spring constants, as

$$K_{tr} = K'_{tr}r_r \quad , \quad C_{tr} = C'_{tr}r_r. \tag{12.4}$$

Introducing a state vector containing the angle and angular velocity for

the tire and rim gives the state space model

$$\begin{pmatrix} \dot{\varphi}_t \\ \dot{\omega}_t \\ \dot{\varphi}_r \\ \dot{\omega}_r \end{pmatrix} = \begin{pmatrix} 0 & 1 & 0 & 0 \\ -\frac{K_{tr}}{J_t} & -\frac{C_{tr}}{J_t} & \frac{K_{tr}}{J_t} & \frac{C_{tr}}{J_t} \\ 0 & 0 & 0 & 1 \\ \frac{K_{tr}}{J_r} & \frac{C_{tr}}{J_r} & -\frac{K_{tr}}{J_r} & -\frac{C_{tr}}{J_r} \end{pmatrix} \begin{pmatrix} \varphi_t \\ \omega_t \\ \varphi_r \\ \omega_r \end{pmatrix} + \begin{pmatrix} 0 & 0 \\ -\frac{1}{J_t} & 0 \\ 0 & 0 \\ 0 & \frac{1}{J_r} \end{pmatrix} \begin{pmatrix} F_{road}r \\ \tau \end{pmatrix}$$

$$y = \begin{pmatrix} 0 & 0 & 0 & 1 \end{pmatrix} \begin{pmatrix} \varphi_t \\ \omega_t \\ \varphi_r \\ \omega_r \end{pmatrix}. \tag{12.5}$$

As seen in the model, the only output from the system is the $\omega_r$ state, because the rim speed is the only value that could be measured.

## 12.2 Simulation of the model

To test the validity of this model, the dynamics was added to the simulation model described in chapter 10. The simulation block in figure 10.2 was changed according to equation 12.5 to include the dynamics described above.

The model introduced new constants, such as $K_{tr}$ and $C_{tr}$. These values were manually tuned to make the simulation model produce results similar to the measured data from the vehicle.

The slip plots produced from the output data of the simulation showed a look similar to the real measured data. Since the results look so much the same, the model was considered fairly correct.

## 12.3 Observer

The wheel speed sensors measure the speed of the rim, but to calculate the slip of the wheel it is more important to know the speed of the tire, since the contact area between the tire and road is the place where the friction force acts.

It would be useful to get an estimate of the angular velocity of the tire based on measurements from the rim. To do this, an observer is used, that tries to estimate the state variables in equation 12.5. The observed value of $\omega_t$ is then used in the slip calculations.

Assuming the system

$$\begin{aligned} \dot{x} &= Ax + Bu \\ y &= Cx, \end{aligned} \tag{12.6}$$

an observer based on the error of the output can be designed as

$$\dot{\hat{x}} = A\hat{x} + Bu + K(y - \hat{y}). \tag{12.7}$$

The error of the observed states is defined as

$$\tilde{x} = x - \hat{x}. \tag{12.8}$$

Rewriting $\hat{x}$ as $\hat{x} = x - \tilde{x}$ and using equation 12.7, gives

$$\dot{x} - \dot{\tilde{x}} = Ax - A\tilde{x} + Bu + KC\tilde{x}, \tag{12.9}$$

which can be simplified to

$$\dot{\tilde{x}} = (A - KC)\tilde{x}. \tag{12.10}$$

It can be noted that the eigenvalues of the matrix $A - KC$ describe the convergence of the observations.

### 12.3.1 Observability and convergence

A check if the system is observable shows that the observability matrix

$$W_o = \begin{pmatrix} C \\ CA \\ CA^2 \\ CA^3 \end{pmatrix} \tag{12.11}$$

does not have full rank and the system is therefore not observable. If the system is detectable, the unobservable states decay to the origin, and their corresponding eigenvalues are less than zero.

The unobservable states are specified by the null space of the observability matrix $W_o$,

$$\text{null}(W_o) = \begin{pmatrix} 1 \\ 0 \\ 1 \\ 0 \end{pmatrix}. \tag{12.12}$$

This shows that the first and third states, corresponding to the tire and rim angles, are unobservable.

Using Maple to determine the eigenvectors for the $A - KC$ matrix gives the results in table 12.1. Some of the expressions for the eigenvalues and eigenvectors are too complicated to write, and are replaced with $\lambda_i$ and $v_{ij}$.

One of the eigenvalues is always locked to zero, which means that there will be no convergence in the direction of the corresponding eigenvector. Since this direction is built up by the two unobservable states, these states do not decay to the origin and the requirements for detectability are not met.

| *Eigenvalue* | *Eigenvector* |
|---|---|
| 0 | $(1, 0, 1, 0)$ |
| $\lambda_2$ | $(v_{21}, v_{22}, 1, v_{24})$ |
| $\lambda_3$ | $(v_{31}, v_{32}, 1, v_{34})$ |
| $\lambda_4$ | $(v_{41}, v_{42}, 1, v_{44})$ |

Table 12.1: Corresponding eigenvalues and eigenvectors for the observer matrix $A - KC$.

What can be noted when looking at the eigenvector corresponding to the eigenvalue zero, is that this eigenvector is linearly independent of the second and fourth states, which are the states corresponding to the angular velocities. The only interesting output from the observer is the tire speed $\omega_t$, and the error in this estimate will converge independently of this eigenvalue.

The eigenvector $(1, 0, 1, 0)$ has also equal values in the first and third state, which means that the steady state error will have the same value for both the tire angle and the rim angle. Taking the difference between these two values will remove the error, so the difference can always be estimated correctly.

### 12.3.2 Modification of the observer

Since it is possible to estimate the difference between the two angles, and the absolute values of the two angles are not interesting, it is not necessary to have to two separate states for the two values. Here a modification of the observer is made, that uses a state for the difference between the two angles. Let $\varphi$ describe the difference,

$$\varphi = \varphi_r - \varphi_t, \tag{12.13}$$

and the state space model will become

$$\begin{aligned}
\begin{pmatrix} \dot{\varphi} \\ \dot{\omega_t} \\ \dot{\omega_r} \end{pmatrix} &= \begin{pmatrix} 0 & -1 & 1 \\ \frac{K_{tr}}{J_t} & -\frac{C_{tr}}{J_t} & \frac{C_{tr}}{J_t} \\ -\frac{K_{tr}}{J_r} & \frac{C_{tr}}{J_r} & -\frac{C_{tr}}{J_r} \end{pmatrix} \begin{pmatrix} \varphi \\ \omega_t \\ \omega_r \end{pmatrix} \\
&\quad + \begin{pmatrix} 0 & 0 \\ -\frac{1}{J_t} & 0 \\ 0 & \frac{1}{J_r} \end{pmatrix} \begin{pmatrix} F_{road}r \\ \tau \end{pmatrix} \\
y &= \begin{pmatrix} 0 & 0 & 1 \end{pmatrix} \begin{pmatrix} \varphi \\ \omega_t \\ \omega_r \end{pmatrix}.
\end{aligned} \tag{12.14}$$

The observability matrix $W_o$ for this system has full rank, and the system is therefore observable. Also, none of the eigenvalues for the matrix $A - KC$ is locked to zero.

Since this simplification results in better properties for the observer, it is the better alternative to use.

### 12.3.3 Discretizing the model

Continuous time has been used when determining which model was the better to use. Since discrete time must be used when implementing the observer, the system in equation 12.6 was discretized using zero order hold in Matlab. The discrete time system is then described by

$$\begin{aligned} x(t+1) &= \Phi x(t) + \Gamma u(t) \\ y(t) &= Cx(t). \end{aligned} \tag{12.15}$$

### 12.3.4 Kalman gain for the observer

The continuous time observer in equation 12.7 has a discrete time equivalence in equation 11.8. In order to use Kalman gain for the observer, the discrete time model has to be expanded with process and measurement noise, according to equation 11.6. The noise processes were assumed to be independent of each other, resulting in that the correlation matrix between the process and measurement noise is equal to zero. The Kalman gain is computed according to the equations in section 11.2.1, and then used in the discrete time observer. The covariance matrices were manually tuned to get rid of the circular look of the slip curves.

### 12.3.5 Verifying the observer

Running the observer requires input vector

$$u = \begin{pmatrix} F_{road}r \\ \tau \end{pmatrix}. \tag{12.16}$$

The brake pressure multiplied with the estimated value of $K_b$ is used as the torque $\tau$. The road force $F_{road}$ is calculated based on equation 2.4.

Running the observer with output from the simulation model produced slip curves again looking as straight lines. This was expected, since the observer was based on the same model as the simulation.

When the observer was used with experimental data, the circular look that existed in the beginning was significantly decreased. Figure 12.4 shows the same test as in figure 12.1 after the data has been filtered through the observer. As can be noted when comparing the figures, the circles of the slip curve are much smaller and it is easier to fit a line through the points to estimate the slope of the curve.

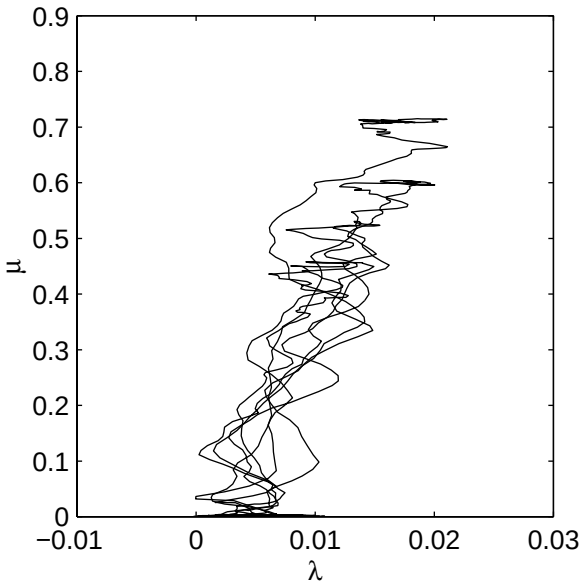


Figure 12.4: Slip curve calculated using observer output.

# Chapter 13

# Classification Part II

Chapter 9 describes the slope estimation of tests taken on dry roads and some taken when water was poured on the pavement. This chapter also looks at some new tests that were carried out, some taken after it had been raining on the road. There are also some new tests with water poured on the road, that did not exist in chapter 9.

The improved algorithms, such as the recursive slope estimation and the elastic tire observer, are in this chapter combined and used for estimating the slope of the surfaces and making a classification between them.

## 13.1 Putting it together

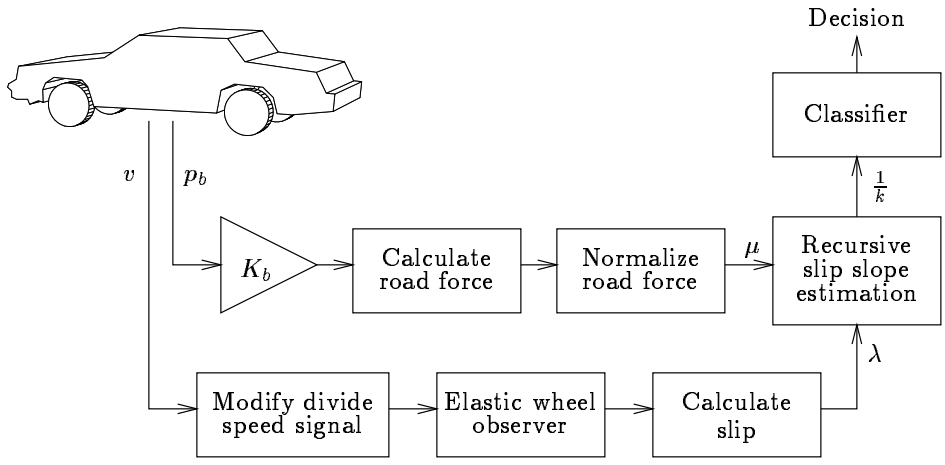


Figure 13.1: Block diagram for the data path from measurements to classification.

When all parts of the data processing are put together, the block diagram in figure 13.1 can be drawn. The figure shows the data path from the car

measurements to the value of the slope at the beginning of the slip curve. A classifier then takes this value and compares it to a threshold in order to make the decision of what kind of surface the road has.

## 13.2 Results

In the tests, the road surfaces are divided into four different categories, see table 13.1. The reason the *Poured1* and *Poured2* categories exist is that

| | |
|---|---|
| *Poured1* | The tests with poured water used in chapter 9 |
| *Poured2* | New tests with poured water on the road |
| *Rain* | Tests after a night's rain, taken when it still was raining |
| *Dry* | Dry asphalt |

Table 13.1: Categories of road surfaces.

they were carried out with a large time interval, and possible differences between them could be studied. Taking these test runs as input to the data processing algorithms gives a series of slope values, where each value corresponds to one test. In figure 13.2 the results are shown for different surfaces. Since the recursive slope estimator works with the inverted slopes, $\frac{1}{k}$, these value are shown in the plot. This makes a line with a low slope, that is leaning to the right in the slip plot, have a position to the right in the figure. Looking at the figure, it can be noticed that the spread between the

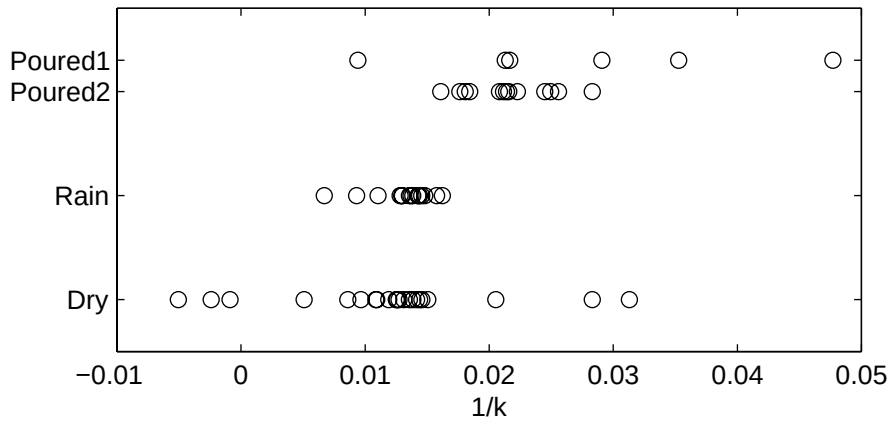


Figure 13.2: Inverted slope for different surfaces.

rain tests is quite small, as well as between the *Poured2* tests. The spread between the dry tests is larger, partly because they were taken at a number

of occasions. When looking at the mean value of the different tests, the dry and rain tests seem to have approximately the same slope, making the surfaces impossible to distinguish between. The big difference is achieved when comparing the tests with poured water to the other surfaces, since the *Poured1* and *Poured2* tests seem to have a smaller slope.

It can look strange that there is a big difference between the road with rain and the road with poured water. The tests marked *Rain* were taken after a whole night of raining. The tests with poured water were taken just after water was poured on a previously dry road. It is conceivable that the difference in the slopes can be explained by that when it first starts to rain on a dry road, the rain will make the dirt and grease on the surface wet, resulting in a slippery surface. After it has been raining a while, the dirt will be washed off the road, making the road cleaner than before. This will reduce the slipperiness of the pavement. Probably the surface will once again have properties similar to the dry road. This could explain why there were not any differences between the dry road and the road wet by rain, since the tests were not performed soon after the rain started. When the water was poured on the road, the road had been dry for quite a while before, which means that there was dirt on the surface.

It would have been useful to have some tests on a road just after beginning of the rain, but there were no opportunities to perform these experiments.

### 13.2.1 Check maximum friction

After examining the slopes for the different surfaces, giving similar values for the rainy road and dry road, it can be questioned what kind of difference there really is between the roads. The goal with the road classification is not just to tell the driver or controller what kind of pavement the road has, but tell what value of friction force can be expected from the contact area between the tire and road.

It can therefore be useful to look at the maximum friction force possible for each of the surfaces. How high deceleration is possible to get before the wheels start to lock up?

The different measurements available to compare for different tests are:

**Accelerometer.** This gives the deceleration of the chassis of the vehicle.

**Torque sensor.** This sensor gives the brake torque of the left front wheel, also useful for looking at the maximum friction force.

**Brake pressure gauges.** These sensors are possible to use, but they can be saturated. They also just measure the brake pressure as it enters the brakes, which is connected to the brake torque with the varying parameter $K_b$.

It turns out that looking at the torque sensor and accelerometer gives the best values for classifying the peak performance of the road.

Looking at the measurements, it is not possible to determine exactly what the maximum friction is. When the wheels lock up, it happens very fast so that process cannot be observed. Since some of the tests were taken with so high brake pressures that the wheel locked up, their values of deceleration and torque can be used as an upper limit, and the tests without the wheel locking up can be used as a lower limit. These limits make up different intervals, which are shown in figure 13.3. According to the figure, as well

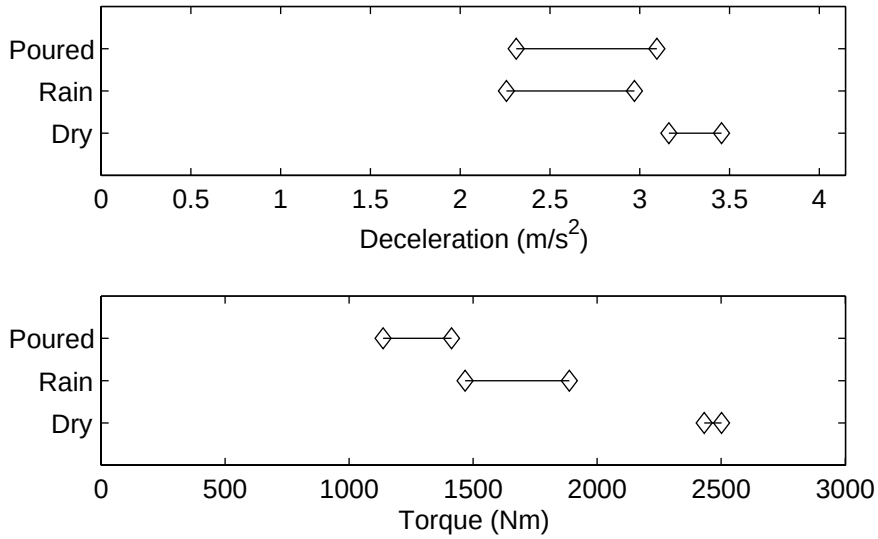


Figure 13.3: Intervals for maximum deceleration and torque, respectively.

the maximum torque as the maximum deceleration for the dry road have higher values than for the two wet categories. It is thus rather clear that the dry road has the highest maximum friction.

The relationship between the two wet types is harder to tell. Looking at the torque plot, the maximum friction for the rainy road seems to be higher than for the road with poured water. Studying the deceleration plot instead, they have overlapping intervals, which means that it is impossible to tell anything from that plot. If the relationship between the rain and poured surfaces in the deceleration plot is true, this would mean that the difference in slopes also had a correspondence in maximum friction force. The intervals in figure 13.3 are based on very few tests, since only the skidding tests and tests with hard braking can be considered. This makes it hard to draw any conclusions about the difference between the two wet types of roads.

## 13.3 Classification

Using the estimated value of the slip slope for a test run, a classifier should give the output of what kind of surface the road has.

The intuitive way to design a classifier to select between two decisions is to compare the value to a threshold and make a selection depending on the outcome of this comparison. Looking at the data values from different tests, a threshold can be selected giving as small error probability as possible.

### 13.3.1 Selecting a threshold between the surfaces

Here, a decision region between the dry road and the road with poured water will be designed. In figure 13.2 these two categories seem to have different slope values and a classifier based on the slope value therefore can be designed.

The spread of the points round the average value is for simplicity modeled as taken from a normal distribution. The variance of the noise is calculated from the data points. Let the type of road be denoted by $x = w$ or $x = d$ for wet and dry roads, respectively. The output from the classifier is called $\hat{x}$.

The existence of a wet road is considered as the 1 bit symbol that should be detected. The bit error probability is then

$$P_b = P_m P(x = w) + P_f P(x = d) \tag{13.1}$$

where

$$P_m = P(\hat{x} = d \mid x = w) \tag{13.2}$$

is the miss probability and

$$P_f = P(\hat{x} = w \mid x = d) \tag{13.3}$$

is the probability for false alarm.

Since the probability of a wet road is not known, they are assumed to $\frac{1}{2}$ each, and equation 13.1 is reduced to

$$P_b = \frac{1}{2}\left(P_m + P_f\right). \tag{13.4}$$

The threshold should be selected as the one minimizing the value of this equation.

The variance and mean of the noise can be estimated from the values of the different tests. Since it is necessary to have some tests for verification of the classifier, all tests cannot be used for making the classifier. In the construction of the classifier, half of the tests are randomly chosen for estimation of the statistic properties, and the rest is used for verification.

### 13.3.2 Error probabilities

Both the *Poured1* and *Poured2* categories are used, and combined into one category of wet tests. Depending on which of the tests are used for determining the decision regions, the results of the verification will become different. Running the procedure several times will create an averaged value that is better to use. The results after running 25000 classifications were

$$\begin{aligned} P_m &= 0.175 \\ P_f &= 0.145 \\ P_b = \frac{1}{2}(P_m + P_f) &= 0.160. \end{aligned}$$

This means that based on these 22 dry and 19 wet tests, there is a probability of 16% of making the wrong decision. With this few tests, values from single tests have big influence. Looking at figure 13.2, the *Poured1* category is very spread out. If for example the value at 0.048 furthest to the right is used when making the decision region, the mean value of the wet surface slopes will get a value to the right and there is an increased miss probability.

If the dry surface is compared only to the *Poured2* category, which is more concentrated round one value, the classifier will work more efficiently. The result after running 25000 classifications was an error probability of only $P_b = 0.123$. This is significantly better than when all wet tests were used, so it can be noted that spread values give a bigger error probability.

The ability to compare tests made at different times is important, since the classifier has to be set up with reference values for different road surfaces and then used for classifying them at a different occasion. Therefore, the first comparison between the dry and all the wet tests is the most important.

# Chapter 14

# Conclusions

## 14.1 Results

Our project had fixed experimental limits, such as the car with its set of sensors and the short test track. This made much of the work consist of dealing with experimental results — not just simulations and theoretical work. The subject was to examine a slip-based method of estimating tire–road friction, using vehicle sensors.

One part of the work consisted of designing a simulation model, helpful for developing the algorithms.

A recursive slip slope estimator based on a method proposed by Gustafsson [Gus95] was implemented for use with our measurements. This estimator made it possible to get real-time updates of the estimated slope values.

An observer that significantly improved the usefulness of the slip data was designed and implemented, based on a model describing the elasticity of the wheel.

A large set of vehicle test data was collected for this project, and these data files can also be useful for future research. The test runs were made on an asphalt road, with either a dry or wet surface. The wet surface could either be accomplished by pouring water on the road or by waiting for rain to fall.

To make decisions between different surfaces a classifier was constructed. This included all the data processing parts described in the work, as well as a decision maker that compared the slip slope to a given threshold. The results were that it was impossible to distinguish between the dry road and the rainy road. A road with rain seemed to have the same slip slope as a dry road, at least when examining the slip curve with these measurements and processing algorithms. However, the duration of the rain seemed important for the slipperiness of the road. When water was poured on a previously dry road, the slope turned out to be different from the dry or rainy road. The difference between the road with poured water and the road with rain could

be explained by that when the water is poured on a dry road, the dirt on the surface will make the road slippery.

An estimation of the error probabilities of a classifier was carried out, using the tests with poured water. Based on a limited number of tests, the error probability of the classifier choosing the wrong surface turned out to be 16%.

An error probability of 16% may seem high, but considering the noisy measurements and the similarity between dry and wet asphalt roads, we are fairly pleased with the result.

## 14.2 Problems — What could have been done different?

A big problem in the work was the noisy measurements from the car. The speed sensors mounted to each wheel was designed for use in the ABS system and automated control. These areas require fast updating, since the control algorithms work with a high sampling frequency. When calculating the difference between two speed values, which is done in the slip calculations, very accurate values of the different wheel speeds are needed. A high sampling frequency is on the other hand not important. If the car was equipped with an other type of sensors, or at least if the data acquisition and filtering in hardware were improved, the results would have been better.

The parameter $K_b$, which describes the scaling between the brake pressure and the torque, varies between the tests and also sometimes within a test. In our algorithms, only one value is used for the whole test. This is a source of errors, so a more trustworthy estimation of $K_b$ would be preferable.

Comparing the properties of two such similar surfaces as dry and wet asphalt was perhaps not a good way to start. If the initial test runs could have been run on surfaces known to be more slippery, we would have been certain that there was a difference between the surfaces, which would have made the development of data processing algorithms easier.

All rain tests were carried out the same day. Taking more tests would have been better, especially if those tests were taken soon after it had started to rain.

## 14.3 Future work

To make the road condition estimation more complete, some of the parallel parts of the project going on right now should also be included:

- The $K_b$ value can be estimated with an adaptive method that do not require the presence of a torque sensor for calibration.

- Instead of using the brake pressure for generating the road force, an observer can be used.

It would also be desirable to be able to brake with all four wheels, and to do this a velocity observer could be developed.

In a future perspective, the communication capabilities of the AHS will be implemented. Then the surface information concerning a certain stretch of the road can be shared between many vehicles.

# Bibliography


[ÅW97] K. J. Åström and B. Wittenmark. *Computer Controlled Systems: Theory and Design.* Prentice Hall, third edition, 1997.

[BER92] B. Breuer, U. Eichhorn, and J. Roth. Measurement of tyre/road-friction ahead of the car and inside the tyre. In *International Symposium on Advanced Vehicle Control*, pages 347–353, 1992.

[Gil92] T. D. Gillespie. *Fundamentals of Vehicle Dynamics.* Society of Automotive Engineers, 1992.

[Gus95] F. Gustafsson. Slip-based estimation of tire–road friction. In *3rd European Control Conference in Rome, Italy*, pages 725–730, 1995.

[PAT] California PATH. Vehicle platooning and automated highways. Fact sheet, available online from http://www.path.berkeley.edu.

[USY94] T. Uno, Y. Sakai, and T. Yamashita. Road surface recognition method using optical spatial filtering. In *International Symposium on Advanced Vehicle Control*, pages 509–515, 1994.

[YHL99] K. Yi, J. K. Hedrick, and S. Lee. Estimation of tire–road friction using observer based identifiers. *Vehicle System Dynamics*, 31(4):233–261, April 1999.

[YJ98] K. Yi and T. Jeong. Observer based estimation of tire–road friction for collision warning algorithm adaptation. *JSME International Journal*, 41(1):116–124, 1998.